

# Disorder-Order Interface Propagating over the Ferromagnetic Ground State in the Transverse Field Ising Chain

Vanja Marić, Florent Ferro, and Maurizio Fagotti  
*Université Paris-Saclay, CNRS, LPTMS, 91405, Orsay, France*  
 (Dated: November 7, 2024)

We consider time evolution of order parameters and entanglement asymmetries in the ferromagnetic phase of the transverse-field Ising chain. One side of the system is prepared in a ferromagnetic ground state and the other side either in equilibrium at higher temperature or out of equilibrium. We focus on the disorder-order interface in which the order parameter attains a nonzero value, different from the ground state one. In that region, correlations follow a universal behaviour. We analytically compute the asymptotic scaling functions of the one- and two-point equal time correlations of the order parameter and provide numerical evidence that also the non-equal time correlations are universal. We analyze the Rényi entanglement asymmetries of subsystems and obtain a prediction that is expected to hold also in the von Neumann limit. Finally, we show that the Wigner-Yanase skew information of the order parameter in subsystems within the interfacial region scales as their length squared. We propose a semiclassical approximation that is particularly effective close to the edge of the lightcone.

## CONTENTS

I. Introduction	1
A. Protocol	2
B. Review of established results	2
II. Results	3
III. GHD at the edge of the lightcone	6
IV. Order parameter correlations	8
A. Universality of the scaling functions	9
B. Approximation of Fredholm determinants	9
C. Numerical checks	10
D. Interfacial region width	13
V. Entanglement asymmetry	13
A. Free-fermion technique	14
B. Conjecture and numerical checks	14
VI. Wigner-Yanase skew information	15
VII. Physical interpretation	16
VIII. Conclusions	18
Acknowledgments	19
References	19

## I. INTRODUCTION

Isolated quantum many-body systems cannot relax as a whole, but they can relax locally in the thermodynamic limit [1, 2]. A compelling argument for this is that the system behaves as its own bath: the lack of information from distant parts of the system can be effectively treated as though the accessible region were coupled to an external reservoir. In integrable one dimensional systems,

such intuition holds true in a rigorous sense. Consider, for instance, the time evolution governed by a translationally invariant Hamiltonian in a system with a thermodynamic Bethe Ansatz description. When the system is bipartitioned, with each half independently prepared either in thermal equilibrium or in the ground state of two potentially different translationally invariant Hamiltonians (with a boundary), its dynamics can be described by generalized hydrodynamics (GHD) [3–10]. The latter consists of integro-differential equations for a type of Wigner functions, which in the specific research field are called “root densities”. The boundary conditions for the GHD equation(s) are not in one-to-one correspondence with the state at the initial time, which, indeed, is not fully characterised by the hydrodynamic quantities. Instead, these boundary conditions reflect the thermodynamic stationary states that describe local observables at late times outside the lightcone spreading from the junction. In other words, the regions outside the lightcone act as an effective reservoir for those inside it.

The aptitude of generalised hydrodynamics to remain unaffected by the details of the initial state, even when those details are complex yet ultimately irrelevant at late times, makes it a very powerful theory. However, this same feature also makes it subject to subtleties that may compromise the completeness of the description, and they are not always immediately apparent. One such issue was recognized shortly after the first GHD proposals: in the easy-axis XXZ spin- $\frac{1}{2}$  chain—an interacting integrable system—the root densities do not determine the sign of the expectation values of operators that are odd under spin-flip [11]. Ref. [12] proposed complementing the root-density characterization with a binary variable to account for the sign of those expectation values. This refined GHD description predicts sharp changes in odd observables over a length scale negligible compared to the typical scale over which the expectation values of even local observables vary. Similar, though distinct, issues also arise in noninteracting models. For example, con-

sider the protocols studied by Eisler and collaborators in Refs [13–15]. Two ground states of a system in an ordered phase are joined, with the underlying symmetry broken in different ways. At late times, the expectation values of local observables become nontrivial functions of the distance from the junction per unit time. What does GHD predict? Nothing. This time the issue is that the root densities are blind to symmetry breaking, hence GHD, as a stand-alone theory, cannot distinguish macroscopically different ground states from one another, and, in turn, is clearly unable to predict the late time behaviour of local observables when two different ground states are joined.

While such issues could be the result of some deficiency in the original GHD description, we argue that they could also signal unusual physical properties of the state. We have indeed recently confirmed our suspicions of anomalous behaviours in the presence of spontaneous symmetry breaking [16, 17]. Specifically, in Ref. [16] we considered the bipartitioning protocol in which a part of the state is prepared in a symmetry breaking ground state and the other in equilibrium at higher temperature. We have shown that both classical and quantum correlations do not cluster inside the interfacial region in which the order parameter varies from zero to the ground state value, and we announced that they are described by universal scaling functions. To understand the anomaly, let  $A_{x(t)}$  be a subsystem centered at  $x(t)$ , whose reduced density matrix can be approximated by that of a homogeneous stationary state  $\rho_{x(t),t}^{\text{st}}$  under a certain criterion of similarity. Ref. [16] suggests that, if  $A_{x(t)}$  is in the interfacial region, it is impossible to choose  $\rho_{x(t),t}^{\text{st}}$  in a way that correctly predicts the behaviour of local observables around  $x(t)$  without incorrectly predicting comparable correlations with observables outside  $A_{x(t)}$ .

We prove here the results announced in Ref. [16] in the specific case of the transverse-field Ising model and extend the analysis to the entanglement asymmetry. We also prove that the late time behaviour is not affected by localized perturbations at the initial time, which is not a priori obvious since the effect of localized perturbations over a symmetry-breaking ground state does not generally fade away [14]. Finally, we investigate quantum correlations using the Wigner-Yanase skew information and propose a semiclassical theory that provides a good approximation of their scaling functions in a particular regime. While our worked example is the two-temperature scenario in the transverse-field Ising chain considered in Ref. [16], we show that the only relevant aspect of the protocol is that half of the initial state is prepared in a symmetry-breaking ground state, provided that the other part exhibits or develops an extensive entropy.

## A. Protocol

The transverse-field Ising chain is described by the Hamiltonian

$$H^{(h)} = - \sum_{\ell} (\sigma_{\ell}^x \sigma_{\ell+1}^x + h \sigma_{\ell}^z), \quad (1)$$

where  $\sigma_{\ell}^{\alpha}$  for  $\alpha = x, y, z$  act as Pauli matrices on site  $\ell$  and as the identity elsewhere;  $h$  parametrises the effect of an external magnetic field in the transverse direction. For  $|h| < 1$  the model exhibits a zero-temperature ferromagnetic phase in which the spin-flip symmetry associated with the transformation  $\prod_j \sigma_j^z$  is spontaneously broken. Namely, for  $|h| < 1$  there are two stable ground states  $|\text{GS}_{\pm}\rangle$  with spontaneous magnetization [18]

$$\langle \text{GS}_{\pm} | \sigma_{\ell}^x | \text{GS}_{\pm} \rangle = \pm m_{\text{GS}}^x, \quad (2)$$

where

$$m_{\text{GS}}^x = (1 - h^2)^{1/8}. \quad (3)$$

For  $|h| > 1$ , instead, the model exhibits a paramagnetic phase in which spins tend to align in the transverse direction.

In most of the paper, we study the bipartitioning protocol in which the system is prepared in a (chiral) equilibrium state for the split Ising Hamiltonian  $H_0^{(h,h)}$ , with  $0 < h < 1$ , in which the coupling between site 0 and 1 is turned off, where

$$H_0^{(h_l, h_r)} = - \sum_{\ell \leq 0} [\sigma_{\ell-1}^x \sigma_{\ell}^x + h_l \sigma_{\ell}^z] - \sum_{\ell > 0} [\sigma_{\ell}^x \sigma_{\ell+1}^x + h_r \sigma_{\ell}^z]. \quad (4)$$

We denote by  $\beta$  the inverse temperature of the left part; the right part is prepared at zero temperature. The spin-flip symmetry is broken on the right hand side, where the longitudinal magnetization (far enough from the boundary) is equal to  $m_{\text{GS}}^x$ . We then consider the local quench consisting in switching on the coupling that was originally off, that is to say, the state time evolves under Hamiltonian (1):  $H_0^{(h_l, h)} \rightarrow H^{(h)}$ .

Alternatively, we consider the global quench in which the left part of the state is prepared in an equilibrium state (e.g., the ground state) of a different Hamiltonian, for example  $H_0^{(h_l, h)} \rightarrow H^{(h)}$ .

## B. Review of established results

Since the two-temperature bipartitioning protocol in the transverse-field Ising chain has been widely investigated, we briefly review some of the results obtained in the past.

The local relaxation to a nonequilibrium steady state was firstly addressed in the framework of  $C^*$  algebra [19], where it was shown, in particular, that, for strictly nonzero temperatures, the stationary state (NESS) capturing the expectation value of local observables in the

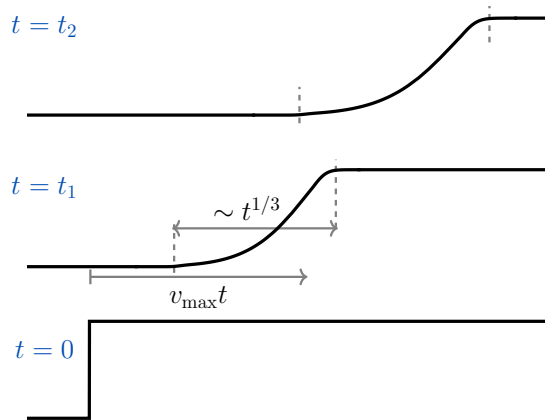


FIG. 1. Schematic representation of the order parameter profile at the initial time  $t = 0$  and two subsequent times  $t = t_1, t_2$  after the quench. The interfacial region moves at the maximal velocity of the quasiparticle excitations and spreads as  $t^{1/3}$ .

limit of infinite time does not depend on the details of the initial state around the junction of the two parts prepared in thermal equilibrium. The same problem was independently studied in Ref. [20] in large but finite chains, and the authors pointed out an emerging scaling limit for the expectation values of the transverse spin, which turned out to become a function of  $\ell/t$ , with  $\ell$  the distance from the junction. They also noted that at the edge of the lightcone the thermal expectation value is approached as  $t^{-1/3}$  over a scale of order  $t^{1/3}$ , but they didn't realise the connection with the Airy kernel introduced by Tracy and Widom a decade before [21]. We also mention Refs [22, 23] that obtained analogous results in other non-interacting systems. To the best of our knowledge, the connection with the Airy kernel in the quantum Ising model was highlighted much later [24, 25]. Some universal aspects of the NESS at the critical point ( $h = 1$  in Eq. (1)) have been pointed out in [26] in the framework of conformal field theory. In particular, the authors computed the energy full counting statistics, showing that, besides the temperatures of the initial state, it depends only on the central charge of the conformal field theory. In a larger collaboration focussed on the quantum Ising chain [27], they confirmed the CFT results and detailed the heat transport and the energy full counting statistics in the paramagnetic phase ( $h > 1$ ). A similar, more extensive, investigation was carried out in Refs [24, 28]. Arguably, [29] is the most complete reference for the expectation value of local operators and equal-time two-point spin correlation functions in the quantum Ising model after the junction of two macroscopically different semi-infinite chains, such as the two-temperature scenario under consideration.

An unsuccessful attempt to reformulate the problem in the framework of phase-space quantum mechanics was reported in [25]. That task was eventually accomplished in [30], which, on the one hand, reinterpreted and enhanced the generalised hydrodynamic equation as the

Schrödinger equation in an invariant manifold, named “locally quasistationary states” after Ref. [31], and, on the other hand, worked out the phase-space formulation of dynamics in noninteracting spin chains starting from Gaussian initial states. The theory was then generalised in Ref. [32] to include non-Gaussian states with spin-flip symmetry. There, Bocini pointed out also some limitations of generalised hydrodynamics on capturing the asymptotic behaviour of connected two-point functions.

The exceptional phenomenology in the presence of spontaneous symmetry breaking had been pointed out in [13, 33]. As far as we can tell, however, such works went almost unnoticed, despite being in apparent conflict with the flourishing theory of generalised hydrodynamics, which, in a noninteracting model like the Ising one, was supposed to provide a complete description of the dynamics. The apparent conflict with GHD is probably more evident when considering the situation later discussed in Ref. [14]. There it was shown that, close to the ground state, the expectation values of local observables at the Euler scale, homeland of generalised hydrodynamics, turn out to be highly sensitive to microscopic details of the initial state that become invisible at mesoscopic scales, making it even unclear how they could be fed into a hydrodynamic equation. The issue of the dependence of the late-time behaviour on the details of the junction of two ground states with spontaneous symmetry breaking has been also recently addressed in Ref. [34] in the continuum scaling limit in which the model can be described by a quantum field theory.

We conclude with a list of features already observed:

- In the limit of large time, the expectation values of spin-flip invariant local observables approach functions of  $\frac{\ell}{t}$ , where  $\ell$  is the position of the observable with respect to the junction.
- The asymptotic behaviour of spin-flip invariant local observables in the limit of large time does not depend on how the initial thermal states have been joined.
- At the edges of the light cone representing the region reached by the information about the junction of the initial thermal states, spin-flip invariant local observables approach their thermal expectation values as  $t^{-\frac{1}{3}}$  over a region of order  $t^{1/3}$ . Their behaviour has an underlying connection with the Airy kernel, which can be understood within the theory of generalised hydrodynamics as a third-order effect in the formal expansion in spatial derivatives [6].

## II. RESULTS

The first aspect we point out is that

**Order is destroyed at the maximal velocity:** This has a very simple interpretation based on the fact

that, in one dimension, order is not expected in a stationary state with extensive entropy.

From Ref. [35] it follows that the entropy of spin blocks is extensive in the limit of infinite time along any ray  $\zeta = \ell/t$  with  $\zeta$  strictly smaller than the maximal velocity of the excitations. Thus, non-symmetric observables can have a nonzero expectation value only starting from around the right edge of the lightcone.

In the initial state that we consider, the transition from ferromagnetic order to disorder is abrupt, but time evolution smooths out the region at the interface. In particular we find

**The width of the interfacial region is  $\sim t^{1/3}$ :** It corresponds to the region in which the behaviour of spin-flip invariant observables is characterised by the Airy kernel.

The interfacial region is schematically represented in Fig. 1. We remark that, while symmetric observables have expectation values close to their values outside the lightcone (the discrepancy is  $O(t^{-1/3})$ ), the expectation value of non-symmetric observables, such as the local longitudinal spin, ranges from 0 to their value in the ground state.

The local longitudinal magnetization  $\langle \sigma^x \rangle$  is the conventional order parameter in the Ising model. In a Gaussian state, it can be reduced to a determinant (in fact, a Pfaffian) of a half-infinite matrix constructed with the elements of the correlation matrix. In the setting we consider the size of the matrix can be effectively reduced because the state is homogeneous outside the lightcone, where the order parameter attains a nonzero value. Close to the right edge of the lightcone such an effective size is then of order  $t^{1/3}$ . This technical insight suggests that  $\langle \sigma^x \rangle$  is highly sensitive only to perturbations to the initial state that alter the elements of the correlation matrix around the right edge of the lightcone at  $O(t^{-\frac{1}{3}})$ . As also discussed in Ref. [6], localised perturbations that keep the initial state Gaussian affect the edge of the lightcone with  $O(t^{-2/3})$  corrections. This leads to one of the most important results of our investigation

**The asymptotics of  $\langle \sigma^x \rangle$  are universal:** they do not depend on microscopic details of the initial state.

The order parameter's profile in the interfacial region depends on the left reservoir only through the density of excitations with the maximal speed. In the thermal case that we consider, this is conveniently parametrized by

$$\eta = -\log \left[ \tanh \left( \frac{\beta \varepsilon(\bar{p})}{2} \right) \right] = -\log \left[ \tanh \left( \beta \sqrt{1 - h^2} \right) \right], \quad (5)$$

where  $\varepsilon(p) = 2\sqrt{1 + h^2 - 2h \cos p}$  is the dispersion relation and  $\bar{p}$  is the momentum of the excitation with maximal speed. We find

$$\langle \sigma_j^x \rangle_t = m_{\text{GS}}^x \mathcal{M}_\eta \left( \frac{j - v_{\text{max}} t}{|t v''(\bar{p})|^{1/3}} \right) + O(t^{-\frac{1}{3}}), \quad (6)$$

where  $v(p) = \varepsilon'(p)$  is the velocity of the quasiparticle excitations with momentum  $p$ ,  $v_{\text{max}} = \max_p v(p)$ , and  $\mathcal{M}_\eta$  is a universal scaling function that depends on the details of the left reservoir only through  $\eta$ . Within the framework of Ref. [36],  $\mathcal{M}_\eta$  could be expressed in terms of the factors of the Wiener-Hopf star factorizations of the symbol

$$a(z, q) = 1 - (1 - e^{-\eta}) \chi(2z + q^2) \quad z, q \in \mathbb{R}. \quad (7)$$

Here  $\chi$  is a primitive of the Airy function,  $\chi(x) = \pi[\text{Ai}(x)\text{Gi}'(x) - \text{Gi}(x)\text{Ai}'(x)]$ , and  $\text{Gi}(x)$  is one of the Scorer functions. Such symbol is however not smooth enough ( $\chi$  is reduced to the Heaviside step function when the star product—cf. (24)—is replaced by the ordinary product), so  $\mathcal{M}_\eta$  cannot be computed within the assumptions of Ref. [36]. We have calculated it within a hybrid perturbation theory where  $\eta$  is identified as the small parameter, but each order of the expansion is computed using an alternative expansion based on the small parameter  $(1 - e^{-\eta})$ . Though unconventional, this method results in a rapidly converging perturbation series as  $\eta \rightarrow 0$  (i.e.,  $\beta \rightarrow \infty$ )—Section IV B

$$\mathcal{M}_\eta(z) \sim \exp \left[ - \sum_{n=1}^{\infty} \eta^n I_n(z) \right]. \quad (8)$$

The first order of the expansion is

$$I_1(z) = \frac{1}{3\pi} \int_0^\infty dy \chi(2z + y^{\frac{2}{3}}), \quad (9)$$

whereas  $I_n(z)$  at higher orders is reported in Section IV. Fig. 2 shows the profile of the longitudinal magnetization as a function of the rescaled variable at different times compared with the perturbative predictions.

Besides the local longitudinal magnetization, we have also studied the entanglement asymmetry [37]  $\Delta S$  of subsystems, which, arguably, quantifies the order as effectively as the “best” odd observable with support in the subsystem. It is defined for a (reduced) density matrix  $\rho_A$  of a (sub)system  $A$  as

$$\Delta S_A = -\text{tr}(\overline{\rho_A} \log \overline{\rho_A}) + \text{tr}(\rho_A \log \rho_A), \quad (10)$$

where  $\overline{\rho_A}$  is the symmetrized reduced density matrix (see section V). For a subsystem  $A = (l, r)$  from site  $l$  to site  $r$  of extent sufficiently larger than the ground-state correlation length, we obtain the following asymptotic behaviour:

$$\Delta S_{(l,r)} = \log 2 - H_1(\mathcal{M}_\eta(z_{r,t})), \quad (11)$$

where  $H_1(x) = -\frac{1+x}{2} \log \frac{1+x}{2} - \frac{1-x}{2} \log \frac{1-x}{2}$ .

This expression is remarkable for two reasons: first, it doesn't depend on the left boundary and, second, it depends on the state only through the one-point scaling function. We do not prove the first property rigorously, but we provide a strong argument in support of it in Section V. On the other hand, assuming the first property, the second one is a direct consequence of the following striking feature:

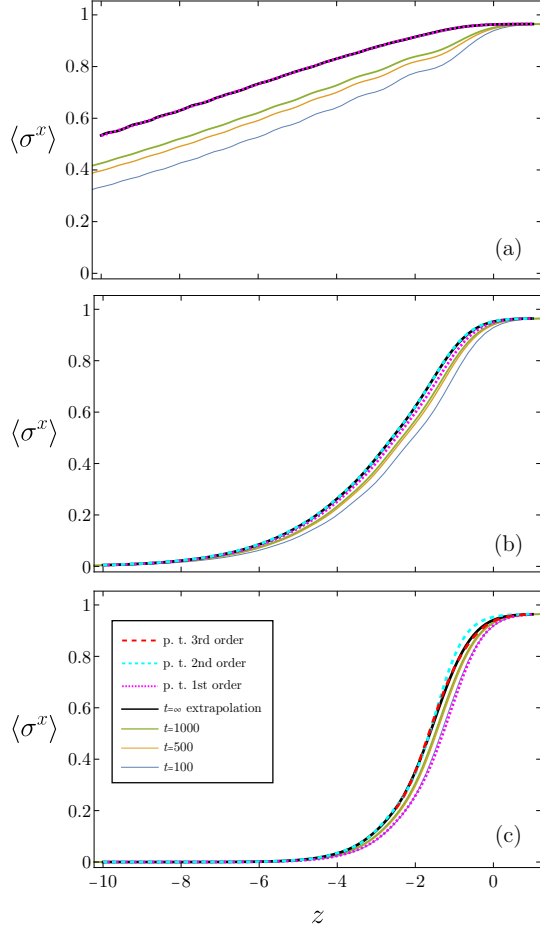


FIG. 2. Magnetization  $\langle \sigma_j^x \rangle$  near the right edge of the lightcone, as a function of  $z = \frac{j-v_{\max}t}{|tv''(\bar{p})|^{1/3}}$ , at different times  $t$  after the quench, including the extrapolation to  $t \rightarrow \infty$ . The magnetic field is set to  $h = 0.5$  and the inverse temperature of the left thermal reservoir is a)  $\beta = 2$ , b)  $\beta = 0.75$ , c)  $\beta = 0.25$ . The data are compared with the predictions at the lowest orders of the perturbation theory.

**Every local order parameter is universal:** the expectation value of any local odd operator  $O_{o,j}$  is characterized by the same scaling function  $\mathcal{M}_\eta(z)$  (with  $z = (j - v_{\max}t)/|tv''(\bar{p})|^{1/3}$ ).

In particular we have

$$\langle O_{o,j} \rangle_t = \langle \text{GS} | O_o | \text{GS} \rangle \mathcal{M}_\eta \left( \frac{j-v_{\max}t}{|tv''(\bar{p})|^{1/3}} \right) + O(t^{-1/3}). \quad (12)$$

Thus, the symbol in eq. (7) fully characterizes the late-time expectation value of local odd observables in the interfacial region where order depletes.

This scaling behaviour is not a peculiarity of one-point functions, indeed also the two point function of the longitudinal spin approaches a function of the rescaled po-

sitions

$$\langle \sigma_j^x \sigma_n^x \rangle_t = (m_{\text{GS}}^x)^2 \mathcal{M}_\eta \left( \frac{j-v_{\max}t}{|tv''(\bar{p})|^{1/3}}, \frac{n-v_{\max}t}{|tv''(\bar{p})|^{1/3}} \right) + O(t^{-1/3}). \quad (13)$$

Using a similar perturbative approach as for the one-point function, we express it as

$$\mathcal{M}_\eta(z_1, z_2) \sim \exp \left[ - \sum_{n=1}^{\infty} \eta^n I_n(z_1, z_2) \right], \quad (14)$$

and we find

$$I_1(z_1, z_2) = I_1(z_1) - I_1(z_2) \quad (15)$$

whereas  $I_n(z_1, z_2)$  for higher  $n$  can be read from the results reported in Section IV. Again, the two point function of any local odd operator at distance  $O(t^{1/3})$  is described by the same scaling function  $\mathcal{M}_\eta(z_1, z_2)$ .

By inspecting just the lowest order of the series expansions for the one- and two-point functions we find

$$\frac{\langle \sigma_j^x \sigma_n^x \rangle_t}{\langle \sigma_j^x \rangle_t \langle \sigma_n^x \rangle_t} = \exp \left[ 2\eta I_1 \left( \frac{n-v_{\max}t}{|tv''(\bar{p})|^{1/3}} \right) + O(\eta^2) \right], \quad (16)$$

which is different from 1 for any ordered pair  $(j, n)$  in the interfacial region, for which  $\langle \sigma_{j,n}^x \rangle \neq 0$ . This is a consequence of the fact that

**The interfacial region is full-range correlated:**

the connected 2-point function of the order parameter is a nonzero function of the rescaled position, hence correlations do not decay inside the interfacial region.

A physical argument in support of this conclusion is that, close to the edge of the lightcone, even if the state is locally very close to the ground state, order is quickly spoiled by the entropy, hence it is reasonable to expect a very large correlation length for odd observables such as the local longitudinal spin. This is witnessed by the scaling of the variance of the total longitudinal spin in any subsystem of the interfacial region. Indeed, let  $S_{(l,r)}^x = \frac{1}{2} \sum_{l \leq \ell \leq r} \sigma_\ell^x$  be the total longitudinal component of the spin between sites  $l$  and  $r$ , whose rescaled positions read  $z_{l,t} = (l - v_{\max}t)/|tv''(\bar{p})|^{1/3}$  and  $z_{r,t} = (r - v_{\max}t)/|tv''(\bar{p})|^{1/3}$ . Let  $\langle S^x, S^x \rangle_c = \langle (S^x)^2 \rangle - \langle S^x \rangle^2$  denote the variance of  $S^x$ . The scaling limit of the one- and two-point functions gives

$$\begin{aligned} \lim_{t \rightarrow \infty} \frac{1}{|v''(\bar{p})t|^{2/3}} \langle S_{(l,r)}^x, S_{(l,r)}^x \rangle_c &= \\ \frac{1}{2} (m_{\text{GS}}^x)^2 \int_{z_l}^{z_r} dy_1 \int_{y_1}^{z_r} dy_2 [\mathcal{M}_\eta(y_1, y_2) - \mathcal{M}_\eta(y_1) \mathcal{M}_\eta(y_2)] \\ &= (m_{\text{GS}}^x)^2 \int_{z_l}^{z_r} dy_1 \int_{y_1}^{z_r} dy_2 e^{-\eta I_1(y_1)} \sinh[\eta I_1(y_2)] + O(\eta^2). \end{aligned} \quad (17)$$

Thus, the variance scales as the square of the subsystem's length, and hence observables at different rescaled variables  $z$  are strongly correlated notwithstanding being at a distance that approaches infinity as  $t \rightarrow \infty$ .

In principle, the extraordinary large variance might just account for strong classical correlations reminiscent of the left thermal reservoir. We show, however, in Sections VI and VII that such a slow decay is not limited to classical correlations, indeed

**The region is in a macroscopic quantum state:**

the Wigner-Yanase skew information  $I_{\rho_A}(S^x)$  in a generic subsystem  $A$  with extent of order  $t^{1/3}$  in the interfacial region scales as the square of the subsystem's length  $|A|$ .

This implies that the size  $\mathcal{N}_A$  of the effective quantum space of  $A$  is proportional to  $|A|$ . Indeed the Wigner-Yanase skew information  $I_{\rho_A}(O)$  provides both a lower bound and an upper bound to the quantum Fisher information  $F_{\rho_A}(O)$ , which is used to bound  $\mathcal{N}_A$  from below [38].

The same concept can be expressed in simpler terms

**The region is full-range quantum correlated:** also the quantum part of the connected correlation of the order parameter does not decay to zero inside the interfacial region.

This readily follows from  $\frac{1}{2}I_{\rho_A}(S^x)$  being a lower bound to the quantum variance introduced in Ref. [39].

For the sake of completeness, Section IV C also exhibits some preliminary numerical data for the (connected) dynamical correlation functions  $\langle \sigma_j^x(t \cos \varphi) \sigma_n^x(\sin \varphi) \rangle_0 - \langle \sigma_j^x(t \cos \varphi) \rangle_0 \langle \sigma_n^x(\sin \varphi) \rangle_0$ , focusing on the case in which sites  $j, n$  correspond to the same scaling variable  $z$ , but at different times, parametrized by  $\varphi \in [\pi/4, \pi/2]$  (i.e.  $|tv''(\bar{p})|^{1/3} z = j - v_{\max} t \cos \varphi = n - v_{\max} t \sin \varphi$ ). We provide numerical evidence that also the non-equal time connected correlations do not approach zero in the limit  $t \rightarrow \infty$  at fixed  $\varphi$

### III. GHD AT THE EDGE OF THE LIGHTCONE

We start with a brief review of the free-fermion techniques useful to deal with Gaussian states that time evolve under the quantum Ising Hamiltonian. We refer the reader to Refs [6, 40] for a more comprehensive review. The Hamiltonian of the transverse-field Ising chain is a quadratic form in the Majorana fermions

$$a_{2\ell-1} = \left( \prod_{j=-\infty}^{\ell-1} \sigma_j^z \right) \sigma_\ell^x, \quad a_{2\ell} = \left( \prod_{j=-\infty}^{\ell-1} \sigma_j^z \right) \sigma_\ell^y, \quad (18)$$

which are self-adjoint operators that satisfy the algebra  $\{a_\ell, a_n\} = 2\delta_{\ell n}I$ . Specifically, the Hamiltonian can be written as  $H = \sum_{j,\ell} a_j \mathcal{H}_{j,\ell} a_\ell / 4$  for some Hermitian anti-symmetric matrix  $\mathcal{H}$ . In the thermodynamic limit  $\mathcal{H}$  is a block-Laurent operator generated by a 2-by-2 symbol  $h(p)$ , that is to say

$$\begin{pmatrix} \mathcal{H}_{2j-1,2\ell-1} & \mathcal{H}_{2j-1,2\ell} \\ \mathcal{H}_{2j,2\ell-1} & \mathcal{H}_{2j,2\ell} \end{pmatrix} = \int_{-\pi}^{\pi} \frac{dp}{2\pi} h(e^{ip}) e^{ip(j-\ell)} \quad (19)$$

with  $h(e^{ip}) = -2\sin(p)\sigma^x - 2(h - \cos(p))\sigma^y$ . The connection with the standard diagonalisation procedure involving a Bogoliubov transformation in the Fourier space is established by the following representation

$$h(e^{ip}) = \varepsilon(p) e^{-i\frac{\theta(p)}{2}\sigma^z} \sigma^y e^{i\frac{\theta(p)}{2}\sigma^z}, \quad (20)$$

where  $\theta(p)$  is the Bogoliubov angle, given by  $e^{i\theta(p)} = -(h - e^{ip})/|h - e^{ip}|$ , and  $\varepsilon(p) = 2\sqrt{1 + h^2 - 2h\cos p}$  is the energy of the quasiparticle excitation with momentum  $p$ .

It is customary to call a state Gaussian if the expectation value of every local operator can be expressed in terms of solely the correlation matrix  $\Gamma_{j,\ell} = \delta_{j,\ell} - \langle a_j a_\ell \rangle$  through the Wick's theorem [41]. If the state is also translationally invariant, its correlation matrix is a block-Laurent operator as well

$$\begin{pmatrix} \Gamma_{2j-1,2\ell-1} & \Gamma_{2j-1,2\ell} \\ \Gamma_{2j,2\ell-1} & \Gamma_{2j,2\ell} \end{pmatrix} = \int_{-\pi}^{\pi} \frac{dp}{2\pi} \Gamma(e^{ip}) e^{ip(j-\ell)}, \quad (21)$$

with a 2-by-2 symbol  $\Gamma(e^{ip})$  [42]. This picture can be extended to inhomogeneous systems by representing the correlation matrix as follows

$$\Gamma_{2j-2+i,2\ell-2+i'} = \int_{-\pi}^{\pi} \frac{dp}{2\pi} [\Gamma_{\frac{i+\ell}{2}}]_{i,i'}(e^{ip}) e^{ip(j-\ell)}, \quad (22)$$

where  $i, i' \in \{1, 2\}$ . Using the terminology of Ref. [36], we say that  $\Gamma$  is a “star-Laurent operator” generated by the symbol  $\Gamma_x(e^{ip})$ . The symbol of the correlation matrix time evolves according to a Moyal dynamical equation, which is decoupled in the following representation [30]

$$\Gamma_{x,t}(e^{ip}) = e^{-i\frac{\theta(p)}{2}\sigma^z} \star \left[ 4\pi \varrho_{x,t;o}(p) + (4\pi \varrho_{x,t;e}(p) - 1)\sigma^y + 4\pi \Psi_{x,t;R}(p)\sigma^z - 4\pi \Psi_{x,t;I}(p)\sigma^x \right] \star e^{i\frac{\theta(p)}{2}\sigma^z}, \quad (23)$$

where  $\varrho_{x,t}(p)$  is the root density,  $\varrho_{e,o} = (\varrho(p) \pm \varrho(-p))/2$  are its even and odd part, respectively, and  $\Psi_{x,t}(p) = \Psi_R(p) + i\Psi_I(p)$  is an auxiliary field, which is odd under  $p \rightarrow -p$ . The operation  $\star$  is the Moyal product, which is formally defined as follows

$$\begin{aligned} (f \star g)(x, p) &= e^{i\frac{\partial_x \partial_q - \partial_y \partial_p}{2}} f(x, p) g(y, q) \Big|_{y=x, q=p} \\ &= \sum_{m,n \in \mathbb{Z}} e^{i(m+n)p} \iint_{-\pi}^{\pi} \frac{d^2 q}{(2\pi)^2} \\ &\quad e^{-i(nq_1 + mq_2)} f(x - \frac{m}{2}, q_1) g(x + \frac{n}{2}, q_2). \end{aligned} \quad (24)$$

As anticipated above, the root density and the auxiliary field have independent dynamical equations: the root density time evolves as a Wigner function

$$i\partial_t \varrho_{x,t}(p) = \varepsilon(p) \star \varrho_{x,t}(p) - \varrho_{x,t}(p) \star \varepsilon(p), \quad (25)$$

whereas the auxiliary field satisfies

$$i\partial_t \Psi_{x,t}(p) = \varepsilon(p) \star \Psi_{x,t}(p) + \Psi_{x,t}(p) \star \varepsilon(-p). \quad (26)$$

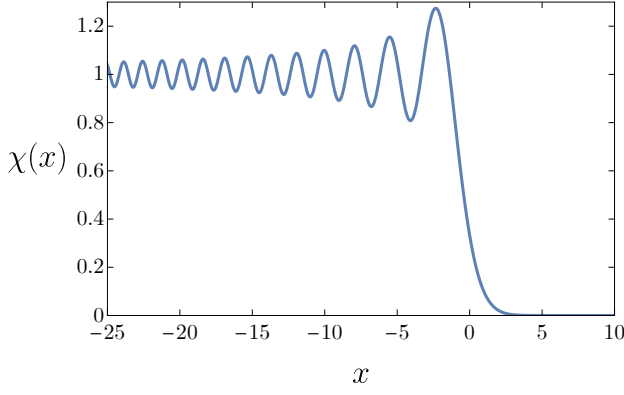


FIG. 3. Function  $\chi$ , appearing in the solution of the third-order GHD equation.

In the limit of low inhomogeneity the Moyal equation can be expanded in the order of space derivatives. Keeping the first two non-zero orders gives the third order generalized hydrodynamic equation

$$\partial_t \varrho_{x,t}^{(3)}(p) + v(p) \partial_x \varrho_{x,t}^{(3)}(p) = \frac{v''(p)}{24} \partial_x^3 \varrho_{x,t}^{(3)}(p), \quad (27)$$

where  $v(p) = \frac{d\varepsilon(p)}{dp}$  is the velocity of the quasiparticle excitation with momentum  $p$ . We remark that the third-order correction is particularly important close to the edge of the lightcone, where it gives a leading contribution [6]. The solution to the third-order GHD equation is readily obtained and reads

$$\varrho_{x,t}^{(3)}(p) = \int_{-\infty}^{\infty} dy \text{Ai}(y) \varrho_{x-v(p)t + \frac{y}{2}[v''(p)t]^{1/3}, 0}^{(3)}(p), \quad (28)$$

where  $\text{Ai}(y)$  is the Airy function. Since it is reasonable to expect that any nonzero entropy density would kill the ferromagnetic order, we focus our attention to the right edge of the lightcone, where the entropy density approaches zero. It is known (and easily deducible from (28)) that the emergent scale around the lightcone is of order  $t^{1/3}$ . Let us then rescale the position in the customary way

$$x = v_{\max} t + |v''(\bar{p})|^{1/3} z_{x,t} t^{1/3}, \quad (29)$$

where  $v(\bar{p}) = v_{\max}$ , and  $z_{x,t}$  is the rescaled position. If  $\varrho_L(p)$  denotes the root density of the left reservoir, we then have

$$\begin{aligned} \varrho_{x,t}^{(3)}(p) &= \varrho_L(p) \theta_H(v''(p)) - \\ &\varrho_L(p) \text{sgn}(v''(p)) \chi \left( 2 \frac{(v(p) - v_{\max}) t^{2/3} - |v''(\bar{p})|^{1/3} z_{x,t}}{[v''(p)]^{1/3}} \right) \end{aligned} \quad (30)$$

where  $\chi$  is the universal Fermi distribution that Refs [43, 44] identified in a degenerate Fermi gas

$$\chi(x) = \int_x^{\infty} dy \text{Ai}[y] = \pi [\text{Ai}(x) \text{Gi}'(x) - \text{Gi}(x) \text{Ai}'(x)], \quad (31)$$

with  $\text{Gi}$  one of the Scorer functions. The function is shown in Fig. 3. We are interested in the infinite time limit of local observables with a finite rescaled position  $z_{x,t} = z$ , i.e., with a position that deviates from the right edge of the lightcone by  $O(t^{1/3})$ . For given  $z$  and fixed momentum  $p$  such that  $v_{\max} - v(p)$  is nonzero,  $\varrho^{(3)}(p)$  approaches zero, which is indicative of the fact that, around the right edge, the state is almost locally equivalent to the ground state. Only excitations with velocity close to the maximal one can be present. Thus, it is convenient to define a rescaled momentum  $q_{p,t}$  representing the displacement from the momentum  $\bar{p}$  with the maximal velocity

$$p = \bar{p} + t^{-1/3} |v''(\bar{p})|^{-1/3} q_{p,t}. \quad (32)$$

At the edge we can find quasiparticles with a finite rescaled momentum  $q_{p,t}$ , indeed the limit of infinite time along the curve  $(z_{x,t}, q_{p,t}) = (z, q)$  is characterised by the following effective root density

$$\varrho_{x,t}(p) \xrightarrow[t \rightarrow \infty]{(z_{x,t}, q_{p,t}) = (z, q)} \varrho_L(\bar{p}) \chi(2z + q^2). \quad (33)$$

In the specific case of a thermal left reservoir, we have

$$\varrho_L(p) = \frac{1}{2\pi} \frac{1}{1 + e^{\beta\varepsilon(p)}}, \quad (34)$$

hence  $\varrho_L(\bar{p}) = (1 - e^{-\eta})/(4\pi)$ , where  $\eta$  was defined in (5). If instead the left hand side is prepared in the ground state of a different noninteracting Hamiltonian,  $\varrho_L(\bar{p})$  is the root density of the GGE describing the stationary values of local observables sufficiently far to the left of the left edge of the lightcone; specifically, it is given by

$$\varrho_L(p) = \frac{1}{2\pi} \sin^2 \left( \frac{\theta(p) - \theta_0(p)}{2} \right), \quad (35)$$

where  $\theta_0(p)$  is the Bogoliubov angle of the prequench Hamiltonian—see, e.g., Ref. [40] for additional details.

So far we have only considered the root density contribution, but what about the auxiliary field? In a bipartitioning protocol in which the right part is initially prepared in a stationary state (such as in the system under consideration), the auxiliary field diffuses around the junction, hence it gives a negligible contribution along any ray with strictly positive slope. Since we are considering the behaviour close the right edge of the lightcone, we can neglect the auxiliary field altogether, which corresponds to projecting the state in the manifold of locally quasistationary states, discussed in Ref. [30], and can be regarded as a hydrodynamic approximation. This observation allows us to regard nonequilibrium preparations of the left part of the chain (resulting in global quenches) as the same as stationary preparations.

In order to reconstruct the symbol of the correlation matrix we should apply the canonical transformation  $(x, p) \rightarrow (z, q)$  to the Bogoliubov angle and to the star product. The star product is unchanged

$$(f \star g)(z_{x,t}, q_{p,t}) = e^{i \frac{\partial_z \partial_\kappa - \partial_\zeta \partial_q}{2}} f(z, q) g(\zeta, \kappa) \Big|_{\substack{\zeta=z \\ \kappa=q}}, \quad (36)$$



where, on the right hand side, the subscripts in  $z$  and  $q$  are understood. For a momentum with velocity close to its maximum, the Bogoliubov angle can be expanded as follows

$$\theta(p) = \theta(\bar{p}) + \theta'(\bar{p})t^{-1/3}|v''(\bar{p})|^{-1/3}q_{p,t} + O(t^{-2/3}). \quad (37)$$

Consequently, every derivative with respect to the rescaled momentum coming from the Moyal product with the Bogoliubov phase in (23) gives an  $O(t^{-1/3})$  contribution, which can be neglected in the limit  $t \rightarrow \infty$ . The Moyal product is therefore reduced to a conventional product, and we can express the symbol of the correlation matrix in the following suggestive way

$$\Gamma_x(e^{ip}) \sim \frac{1-e^{-\eta}}{2} \left[ \chi(2z_x + q_p^2) - \chi(2z_x + q_{-p}^2) \right] \text{I} + \left[ 1 - \frac{1-e^{-\eta}}{2} (\chi(2z_x + q_p^2) + \chi(2z_x + q_{-p}^2)) \right] \Gamma_{\text{GS}}(e^{ip}), \quad (38)$$

where the time dependence is understood and  $\Gamma_{\text{GS}}(e^{ip}) = -\sigma^y e^{i\theta(p)\sigma^z}$  is the symbol of the ground state's correlation matrix.

We remark that, if we take the infinite time limit along the curve  $(z_{x,t}, q_{\pm p,t}) = (z, \pm q)$ , the symbol of the correlation matrix commutes with the symbol of the Laurent operator associated with the Hamiltonian. This confirms that, at the level of the correlation matrix, the infinite time limit along the curve  $z_{x,t} = z$  is locally described by a stationary state.

#### IV. ORDER PARAMETER CORRELATIONS

While local observables that are even under spin flip can be computed using the Wick's theorem based on the homogeneous correlation matrix (38) with  $z_{x,t} = z$ , odd observables have a semilocal fermionic representation (cf. (18)) and depend on the half-infinite correlation matrix whose corner corresponds to the position of the operator. For example, let us consider the typical order parameter of the quantum Ising model, i.e., the local longitudinal magnetization. By the Lieb-Robinson bounds [45], we can compute the one-point function of the order parameter from its two-point function with an operator located far to the right of the lightcone (see also Refs [31, 46])

$$\langle \sigma_\ell^x \rangle_t = \lim_{n \rightarrow \infty} \frac{\langle \sigma_\ell^x \sigma_n^x \rangle_t}{\langle \sigma^x \rangle_{\text{GS}}}. \quad (39)$$

The two point function is proportional to the Pfaffian of the matrix obtained by removing the first row and column from the correlation matrix of the subsystem  $(\ell, \infty)$ , which we call  $\Gamma^{xx}$ . Specifically, we have

$$\langle \sigma_\ell^x \sigma_n^x \rangle = i^{n-\ell} \text{Pf}[\Gamma_{(\ell,n)}^{xx}], \quad (40)$$

where  $\Gamma_{(\ell,n)}^{xx}$  is the finite section of  $\Gamma^{xx}$  from site  $2\ell - 1$  to  $2n$ . For a “star block-Toeplitz matrix” (an inhomogeneous semi-infinite matrix, as dubbed in Ref. [36]) generated by a 2-by-2 symbol such as (38), removing the first

row and column is equivalent to transforming the symbol as follows

$$\Gamma_x(e^{ip}) \equiv \begin{pmatrix} [\Gamma_x(e^{ip})]_{11} & [\Gamma_x(e^{ip})]_{12} \\ [\Gamma_x(e^{ip})]_{21} & [\Gamma_x(e^{ip})]_{22} \end{pmatrix} \mapsto \begin{pmatrix} [\Gamma_x(e^{ip})]_{22} & e^{ip}[\Gamma_{x+\frac{1}{2}}(e^{ip})]_{21} \\ e^{-ip}[\Gamma_{x+\frac{1}{2}}(e^{ip})]_{12} & [\Gamma_{x+1}(e^{ip})]_{11} \end{pmatrix} \equiv \Gamma_x^{xx}(e^{ip}). \quad (41)$$

Importantly,  $\Gamma_{x,t}(e^{ip})$  in (38), and hence  $\Gamma_{x,t}^{xx}(e^{ip})$  in (41), is different from the symbol of the ground state correlation matrix only for an  $O(1)$  phase-space region (i.e., for  $x$  in the interfacial region, which is  $O(t^{1/3})$ , and  $p$  close to the momentum with the maximal velocity, which is  $O(t^{-1/3})$ ). An  $O(t^{-1/3})$  correction confined in the same region does not affect the asymptotic behaviour of the Pfaffian, hence we can confuse positions  $x + \frac{1}{2}$  and  $x + 1$  with  $x$  and simplify the transformation in  $\Gamma_{x,t}^{xx}(e^{ip}) \sim e^{i\frac{p}{2}\sigma^z} \sigma^x \Gamma_{x,t}(e^{ip}) \sigma^x e^{-i\frac{p}{2}\sigma^z}$ , where we also used  $\text{tr}[\Gamma_{x,t}(e^{ip})\sigma^z] = 0$ . Thus we have

$$\Gamma_x^{xx}(e^{ip}) \sim \frac{1-e^{-\eta}}{2} \left[ \chi(2z_x + q_p^2) - \chi(2z_x + q_{-p}^2) \right] \text{I} + \left[ 1 - \frac{1-e^{-\eta}}{2} (\chi(2z_x + q_p^2) + \chi(2z_x + q_{-p}^2)) \right] \Gamma_{\text{GS}}^{xx}(e^{ip}). \quad (42)$$

In our setting the one-point function has the sign of the order parameter in the ground state prepared on the right hand side of the junction, which we agreed to be positive, hence we can write

$$\lim_{n \rightarrow \infty} \frac{\langle \sigma_\ell^x \sigma_n^x \rangle_t}{(m_{\text{GS}}^x)^2} = \exp \left[ \frac{1}{2} \text{tr} \left( \log \left( (\Gamma_{\text{GS}(\ell,\infty)}^{xx})^{-1} \Gamma_{(\ell,\infty)}^{xx} \right) \right) \right] \quad (43)$$

where we isolated the ground state contribution. The symbol of the product of two Toeplitz operators is not the product of their symbols; and a similar result holds true for inhomogeneous matrices. The error in carrying products and inverse at the level of symbols for an operator with a smooth symbol without zeros, such as  $\Gamma_{\text{GS}(\ell,\infty)}^{xx}$ , is however quasilocalised around the corner of the matrix, which is negligible in the scaling limit under consideration. Thus we have

$$\lim_{n \rightarrow \infty} \frac{\langle \sigma_\ell^x \sigma_n^x \rangle_t}{(m_{\text{GS}}^x)^2} = e^{\frac{1}{2} \text{tr} \left( \log \left( \text{I} - W_{(\ell,\infty)}^{(+)} \frac{\text{I} + \Gamma_{\text{GS}(\ell,\infty)}^{xx}}{2} - W_{(\ell,\infty)}^{(-)} \frac{\text{I} - \Gamma_{\text{GS}(\ell,\infty)}^{xx}}{2} \right) \right)} \quad (44)$$

where  $W^\pm$  are generated by the scalar symbols

$$W_x^{(\pm)}(e^{ip}) = (1 - e^{-\eta}) \chi(2z_{x,t} + q_{\mp p,t}^2). \quad (45)$$

We can use the same argument as before to infer that  $\frac{\text{I} \pm \Gamma_{\text{GS}(\ell,\infty)}^{xx}}{2}$  can be treated as projectors

$$\frac{\text{I} + s\Gamma_{\text{GS}(\ell,\infty)}^{xx}}{2} \frac{\text{I} + s'\Gamma_{\text{GS}(\ell,\infty)}^{xx}}{2} \approx \delta_{ss'} \frac{\text{I} + s\Gamma_{\text{GS}(\ell,\infty)}^{xx}}{2}, \quad (46)$$



with  $s, s' = \pm 1$ . Since  $W^+$  and  $W^-$  are equivalent and the scaling variables are such that sums over indices can be turned into integrals up to corrections  $O(t^{-1/3})$ , we can finally express the local longitudinal magnetization as a Fredholm determinant

$$\langle \sigma_\ell^x \rangle_t \sim m_{\text{GS}}^x \det [\mathbf{I} - (1 - e^{-\eta}) \hat{n}_{z_{\ell,t}}] , \quad (47)$$

where

$$\hat{n}_{z_0}(z_1, z_2) = \int_{-\infty}^{\infty} \frac{dq}{2\pi} \chi(2z_0 + z_1 + z_2 + q^2) e^{iq(z_1 - z_2)} \quad (48)$$

and  $z_1, z_2 \geq 0$ .

The two-point function has an analogous expression with respect to a finite section of the operator  $\hat{n}_{z_0}$

$$\langle \sigma_\ell^x \sigma_n^x \rangle_t \sim (m_{\text{GS}}^x)^2 \det [\mathbf{I} - (1 - e^{-\eta}) \hat{n}_{z_{\ell,t}, z_{n,t}}] \quad (49)$$

where  $\hat{n}_{z_{\ell,t}, z_{n,t}}(z_1, z_2) = \hat{n}_{z_{\ell,t}}(z_1, z_2)$  for  $z_{\ell,t} < z_1, z_2 < z_{n,t}$  (and 0 otherwise).

### A. Universality of the scaling functions

Even if we derived (47) and (49) focusing on the local longitudinal spin, we point out that most of the changes associated with replacing  $\sigma_\ell^x$  by another odd local observable are subleading. The reason is that the expectation value of any odd local observable that can be written as the product of Pauli matrices is represented by a Pfaffian of a matrix that is identical to  $\Gamma_{(\ell,n)}^{(xx)}$  except for a finite number of rows and columns. The latter affects the asymptotic expression only through the expectation value of the operator in the ground state. Specifically we find

$$\begin{aligned} \langle O_x \rangle_t &\sim \langle O \rangle_{\text{GS}} \det [\mathbf{I} - (1 - e^{-\eta}) \hat{n}_{z_{x,t}}] \\ \langle O_x O'_y \rangle_t &\sim \langle O \rangle_{\text{GS}} \langle O' \rangle_{\text{GS}} \det [\mathbf{I} - (1 - e^{-\eta}) \hat{n}_{z_{x,t}, z_{y,t}}] , \end{aligned} \quad (50)$$

where  $O, O'$  are odd local observables at a finite rescaled distance from each other. Following the same reasoning, we also argue

$$\langle O_x E_y \rangle_t \sim \langle O \rangle_{\text{GS}} \langle E \rangle_{\text{GS}} \det [\mathbf{I} - (1 - e^{-\eta}) \hat{n}_{z_{x,t}}] , \quad (51)$$

where  $E$  is an even local observable at a finite rescaled distance from  $O$  ( $y$  can be either greater or less than  $x$ ). At a finite rescaled distance, instead, local observables that are even under spin flip cluster and approach the ground-state expectation values.

Incidentally, a similar reasoning applies to non-equal time two-point functions. In particular, we argue

$$\frac{\langle O_x(t \cos \phi) O_y(t \sin \phi) \rangle_0}{\langle O'_x(t \cos \phi) O'_y(t \sin \phi) \rangle_0} \sim \frac{\langle O \rangle_{\text{GS}}^2}{\langle O' \rangle_{\text{GS}}^2} , \quad (52)$$

where 0 stands for the initial state. Because of (50), the same result applies also to the connected part of the correlation function.

The second sign of universality that we would like to point out comes from having characterised the left reservoir through a single parameter,  $\eta$ . Such a simplification is particularly strong if we take into account that our derivation is not specific to thermal reservoirs. Indeed, the left part of the initial state is characterised by a single parameter even if it is prepared in a generalised Gibbs ensemble, or in a nonequilibrium state. For instance, Fig. 5 shows an example in which the left hand side of the chain is prepared in the ground state of the Ising model in a different magnetic field.

The third aspect of universality is that the scaling functions are also stable under localised perturbations. This can be shown as follows. Let  $B^L = (B^L)^\dagger$  be the boundary edge mode of the model, which is an odd conserved involution with support quasilocalised around the left boundary of the right semi-infinite chain (see, e.g., Ref. [47]) and satisfying  $B^L |\text{GS}\rangle = |\text{GS}\rangle$ . We consider the effect of applying to the initial state a unitary transformation  $U$ , with support quasilocalised around the junction. We can always decompose  $U$  as follows:

$$U = W_+ + W_- B^L , \quad (53)$$

where  $W_\pm$  are even under spin flip. Since the symmetry-breaking ground state is an eigenstate of  $B^L$ ,  $U$  can be replaced by  $W = W_+ + W_-$ . Thus we have

$$\begin{aligned} \text{tr}(e^{-iHt} U [\rho_\beta \otimes |\text{GS}\rangle\langle\text{GS}|] U^\dagger e^{iHt} \sigma_\ell^x \sigma_n^x) = \\ \text{tr}(e^{-iHt} W [\rho_\beta \otimes \rho_\infty] W^\dagger e^{iHt} \sigma_\ell^x \sigma_n^x) , \end{aligned} \quad (54)$$

where we denoted the Gibbs ensemble with inverse temperature  $\beta$  by  $\rho_\beta$  and we allowed ourselves to replace  $|\text{GS}\rangle\langle\text{GS}|$  by  $\rho_\infty$  because  $W$  is even under spin flip. Being quasilocal and even,  $W$  can be approximated by a finite sum of Gaussians with support quasilocalised around the junction. The contribution from each of these Gaussians is captured by a pair of root density and auxiliary field that differs from the one without  $U$  only in the neighborhoods of the junction. As discussed in Ref. [6], such perturbations affect the edge of the lightcone at  $O(t^{-2/3})$  and are therefore negligible in the scaling limit that we consider.

The fourth aspect of universality that we would like to emphasize is that the scaling functions are not specific to the transverse-field Ising chain. We chose the model only for its simplicity and notoriety, but the same formulas apply, in particular, to any quantum spin chain that can be mapped to free fermions by a Jordan-Wigner transformation, such as the quantum XY model, provided to be in a phase with spontaneous symmetry breaking. Minor changes are expected only when there is more than one mode associated with the maximal velocity, such as in the quantum XY model without external field.

### B. Approximation of Fredholm determinants

The limit of low temperature (or of small quench, in the sense of Ref. [48]) corresponds to the limit  $\eta \rightarrow 0$ , and

$1-e^{-\eta}$  presents itself as the natural small parameter in the trace expansion of the Fredholm determinant. On the other hand, the logarithm of the determinant is mainly determined by the eigenvalues of  $\hat{n}_z$  that are close to 1 (note that  $\hat{n}_{-\infty}$  is an involution), for which  $\eta$  is the natural parameter of the expansion. Thus, we consider the set of polynomials  $p_n$  generated by

$$-\log(1 - (1 - e^{-w})x) = \sum_{n=1}^{\infty} w^n p_n(x)$$

and define

$$\begin{aligned} I_n(z) &= \text{tr}(p_n(\hat{n}_z)) \\ I_n(z_1, z_2) &= \text{tr}(p_n(\hat{n}_{z_1, z_2})) \end{aligned} \quad (55)$$

We mention that such polynomials satisfy  $p_n(x) = (-1)^n p_n(1-x)$  and report the first of them

$$\begin{aligned} p_1(x) &= x \\ p_2(x) &= \frac{1}{2}(x^2 - x) \\ p_3(x) &= \frac{1}{6}(2x^3 - 3x^2 + x) \\ p_4(x) &= \frac{1}{24}(6x^4 - 12x^3 + 7x^2 - x) \end{aligned} \quad (56)$$

The one- and two-point scaling functions are then given by

$$\begin{aligned} \det[\mathbb{I} - (1 - e^{-\eta})\hat{n}_z] &= \exp\left(-\sum_{n=1}^{\infty} \eta^n I_n(z)\right) \\ \det[\mathbb{I} - (1 - e^{-\eta})\hat{n}_{z_1, z_2}] &= \exp\left(-\sum_{n=1}^{\infty} \eta^n I_n(z_1, z_2)\right) \end{aligned} \quad (57)$$

We observe that these series are rapidly convergent for generic  $z$  even at rather high temperature, therefore we can use the finite sums of the first few terms of the series as excellent approximations of the asymptotic behaviour. Since the contribution from  $I_2(z)$  starts being visible for  $\beta \lesssim 1$ , we report an integral representation that can be evaluated numerically without special precautions

$$\begin{aligned} I_2(z) &= \frac{1}{2} \left[ \iint_{-\infty}^{\infty} \frac{dq_1 dq_2}{(2\pi)^2} \iint_z^{\infty} dy_1 dy_2 e^{i(q_1 - q_2)(y_1 - y_2)} \right. \\ &\quad \left. \chi(y_1 + y_2 + q_1^2) \chi(y_1 + y_2 + q_2^2) \right] - \frac{1}{2} I_1(z) \end{aligned} \quad (58)$$

Functions  $I_1$  and  $I_2$  are shown in Fig. 4.

### C. Numerical checks

We have compared our analytical predictions against numerical data considering time evolution in a finite-size system with open boundary conditions. We employed standard methods based on the mapping to free fermions.

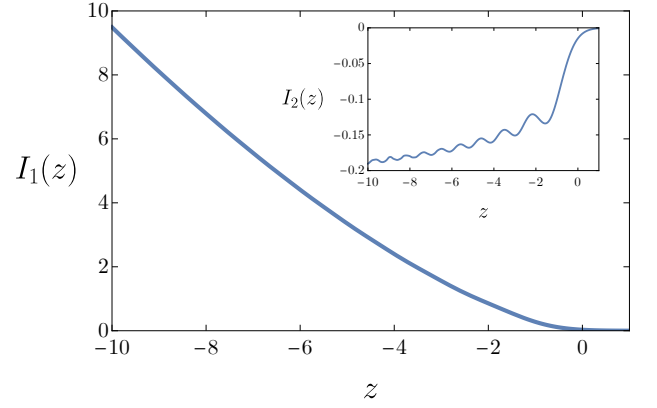


FIG. 4. Functions  $I_1$  (main plot) and  $I_2$  (inset), appearing in the expansion of the Fredholm determinant.

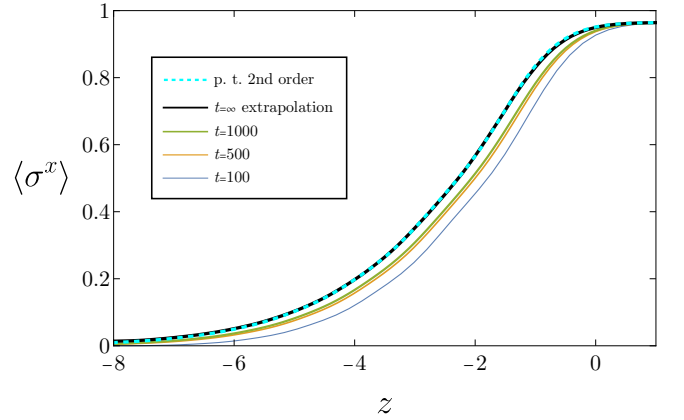


FIG. 5. The same as in Fig. 2, except that the left part of the system is prepared in the ground state of the model with  $h = 2$  (paramagnetic phase), rather than in an equilibrium state.

*a. One-point function.* In Fig. 2 we report the time evolution of the magnetization  $\langle \sigma_j^x \rangle$  as a function of the rescaled variable  $z_{j,t} = \frac{j - v_{\max} t}{|tv''(\bar{p})|^{1/3}}$ , for several different temperatures of the left thermal reservoir. Assuming corrections of the form  $at^{-1/3} + bt^{-2/3}$ , for some coefficients  $a, b$ , we extrapolate the results to  $t \rightarrow \infty$ . The extrapolated limit is in excellent agreement with prediction (8), which we approximate by replacing the series with a finite sum of a sufficiently large number of terms. Since the parameter of the perturbation theory increases with temperature, for a left reservoir at higher temperature, a higher number of terms is required.

In Fig. 5 we present an analogous study where the left part of the system is prepared out of equilibrium in the ground state of the Ising model with a different magnetic field within the paramagnetic phase. Again, the agreement with the prediction is excellent. In Fig. 6 we show the alternative order parameter  $\langle \sigma_j^x \sigma_{j+2}^z \rangle$ , confirming the universality of the scaling function (12), in that it is not specific to the longitudinal magnetization.

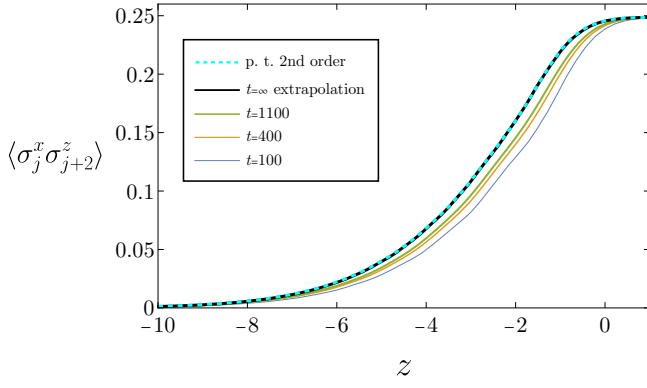


FIG. 6. The same as in Fig. 2, but for the order parameter  $\langle \sigma_j^x \sigma_{j+2}^z \rangle$ , and only for  $\beta = 0.75$ .

*b. Two-point function.* We find excellent agreement also with our predictions for the order parameter two-point function. For instance, Fig. 7 shows the increase of the variance of the longitudinal component of the total spin in the semi-infinite subsystem—in the right edge comoving frame—whose (left) boundary corresponds to rescaled variable  $z$ . Specifically, with a slight abuse of notations, we denote  $\frac{1}{2} \sum_{\ell \geq j} \sigma_\ell^x$  by  $S^x$ , and  $\frac{j-v_{\max}t}{|tv''(\bar{p})|^{1/3}}$  by  $z$ . We then consider the difference

$$\Delta \langle S^x, S^x \rangle_c = \langle S^x, S^x \rangle_{c,t} - \langle S^x, S^x \rangle_{c,\text{GS}}, \quad (59)$$

where  $\langle S^x, S^x \rangle_{c,t} = \langle (S^x)^2 \rangle_t - \langle S^x \rangle_t^2$  is the variance of  $S^x$  at time  $t$  and  $\langle S^x, S^x \rangle_{c,\text{GS}}$  is its variance in the ground state. We have subtracted the latter so as to remove the divergency of the variance. Note that, setting the right boundary of the subsystem to a rescaled position  $z_r \sim 1$  would introduce just exponentially small corrections in  $z_r$  (the state becomes indistinguishable from the ground state at a positive large enough rescaled position). Thus, the effective size of the subsystem is not infinite but rather scales as  $|v''(\bar{p})t|^{1/3}$ . Since the ground state variance would then scale as  $|v''(\bar{p})t|^{1/3}$ , by computing  $\lim_{t \rightarrow \infty} \frac{1}{|v''(\bar{p})t|^{2/3}} \Delta \langle S^x, S^x \rangle_c$  we are accessing the asymptotics of the variance in a subsystem including the edge of the lightcone. In particular, we can extract the first order of the perturbation theory from eq. (17)

$$\lim_{t \rightarrow \infty} \frac{1}{|v''(\bar{p})t|^{2/3}} \Delta \langle S^x, S^x \rangle_c = (m_{\text{GS}}^x)^2 \int_z^\infty dy_1 \int_{y_1}^\infty dy_2 e^{-\eta I_1(y_1)} \sinh[\eta I_1(y_2)]. \quad (60)$$

We have compared this prediction with the extrapolation of our data to  $t \rightarrow \infty$ . As for the one-point function, the lower the temperature of the left reservoir, the better the agreement. To correctly capture the asymptotics at higher temperatures would require retaining higher orders of the perturbation theory.

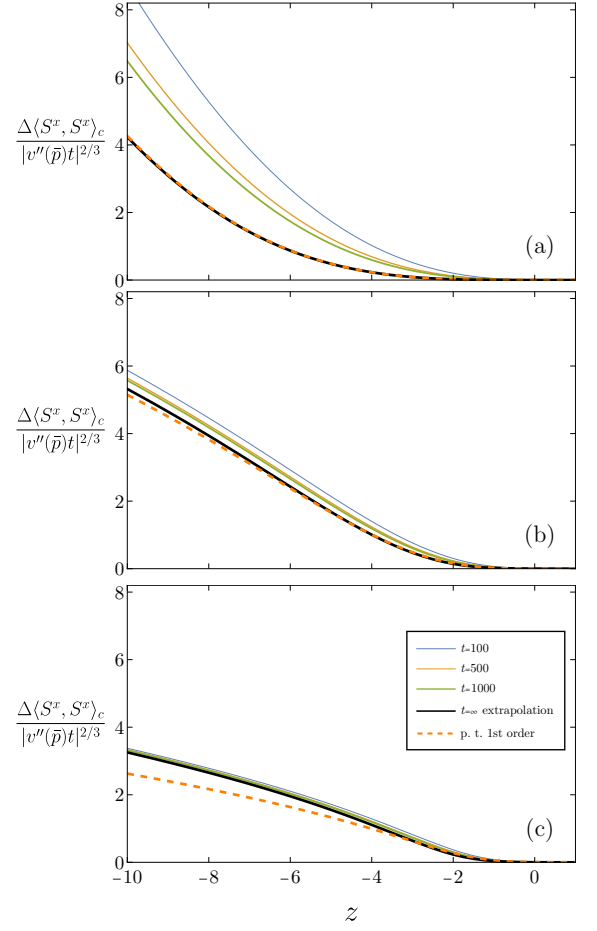


FIG. 7. Difference between the variance of  $S^x = \frac{1}{2} \sum_{\ell \geq j} \sigma_\ell^x$  after the quench and the same variance in the ground state of the model, as a function of the rescaled position  $z = (j - v_{\max}t)/|tv''(\bar{p})|^{1/3}$ , at different times  $t$  with a)  $\beta = 2$ , b)  $\beta = 0.75$ , c)  $\beta = 0.25$ . The other parameters are the same as in Fig. 2.

*c. Stability.* We have tested the resilience of the late-time behaviour of the one-point function to localised perturbations in the initial state. To that aim, we have quantified the deviation from the clean case as follows

$$D(z_{j,t}) \equiv \frac{\langle \sigma_j^x(t) \rangle_0 - \frac{\langle e^{i\alpha_1 \sigma_1^z} \sigma_j^x(t) e^{i\alpha_2 \sigma_1^y \sigma_2^y} \rangle_0}{\langle e^{i\alpha_1 \sigma_1^z} e^{i\beta \sigma_1^y \sigma_2^y} \rangle_0}}{m_{\text{GS}}^x \mathcal{M}(z_{j,t})}, \quad (61)$$

where 0 stands for the initial state, and we have normalised the difference by the asymptotic magnetization in the limit  $t \rightarrow \infty$ . The data for  $\alpha_1 = 2\alpha_2 = 1$  are reported in Fig. 8, where we have grouped the points in bins and made a fit with corrections  $t^{-1/3}$ . We have attached an error  $t^{-2/3}$  to the data so as to effectively capture the subleading orders of the asymptotic expansion in the limit of infinite time. The error on the rescaled position is artificial and represents the width of the bins used. The error bars on  $D$  correspond to the 95% confidence interval on the estimation of the parameters of the fit, which should

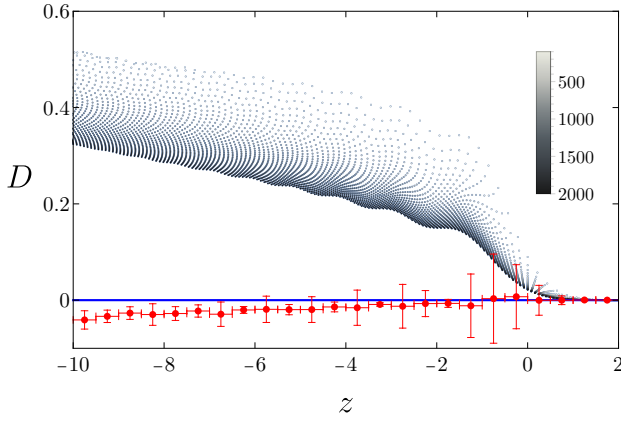


FIG. 8. The quantity  $D_j$ , defined in Eq. (61), with  $\alpha_1 = 2\alpha_2 = 1$ , as a function of the rescaled position  $z = (j - v_{\max}t)/|tv''(\bar{p})|^{1/3}$ . Different times  $t$  are indicated by different shades of gray (legend). The extrapolation to  $t \rightarrow \infty$  is represented by red points, and the zero value by a solid blue line. The parameters of the model are  $h = 0.5, \beta = 0.75$ .

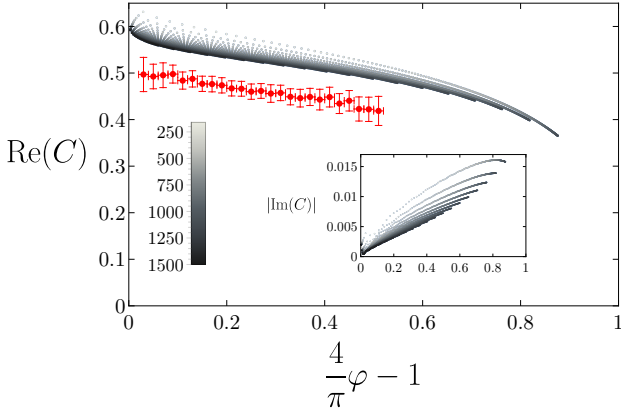


FIG. 9. Dynamical connected correlation function  $C \equiv \langle \sigma_j^x(t \cos \varphi) \sigma_\ell^x(t \sin \varphi) \rangle - \langle \sigma_j^x(t \cos \varphi) \rangle \langle \sigma_\ell^x(t \sin \varphi) \rangle$ , at fixed rescaled position  $z = -2$  ( $z = (j - v_{\max}t \cos \varphi)/|tv''(\bar{p})|^{1/3} = (\ell - v_{\max}t \sin \varphi)/|tv''(\bar{p})|^{1/3}$ ) with  $\beta = 0.75, h = 0.5$ . The main plot and the inset display the real part and the imaginary part, respectively. Different shades of gray correspond to different values of  $t$ , as indicated in the legend. The extrapolation to  $t \rightarrow \infty$  is represented by red points.

be regarded just as a suggestive estimation. Considering that the larger  $-z$  and the larger  $t$  are expected to be the asymptotic corrections, we conclude that the extrapolation to  $t \rightarrow \infty$  is consistent with the prediction. This, in turn, supports the stability of the result under localised perturbations in the initial state.

*d. Non-equal time correlations.* While our theoretical analysis has been focussed on equal-time correlations, we think that non-equal time correlations play a role that is too important to be completely overlooked. In equilibrium, the weak clustering of local observables across different times is an inherent part of its definition [49].

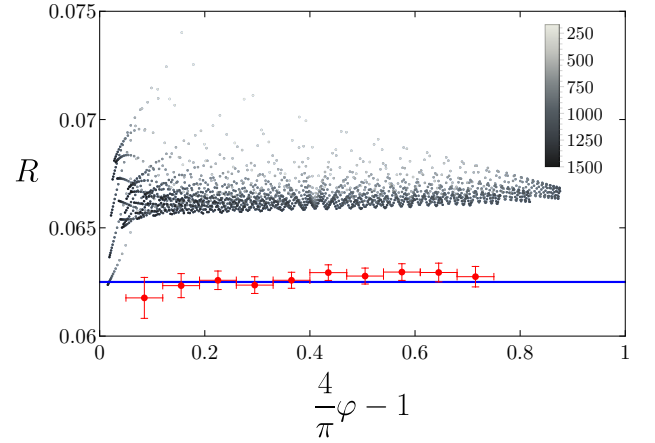


FIG. 10. Ratio (63), with  $O_j = \sigma_j^x \sigma_{j+1}^z$  and  $(t_1, t_2) = (t \cos \varphi, t \sin \varphi)$ , at fixed scaling variable  $z = -2$  ( $z = (j - v_{\max}t_1)/|tv''(\bar{p})|^{1/3} = (\ell - v_{\max}t_2)/|tv''(\bar{p})|^{1/3}$ ) with  $\beta = 0.75, h = 0.5$ . Different shades of gray correspond to different values of  $t$ , as indicated in the legend. The extrapolation to  $t \rightarrow \infty$  is represented by red points, while the solid blue line is the prediction  $R = \langle O \rangle_{\text{GS}}^2 / \langle \sigma^x \rangle_{\text{GS}}^2$ .

In our specific case in which relaxation occurs along a space-time curve, we find it natural to wonder what happens to non-equal time correlations in the limit of infinite time at fixed rescaled position  $z$  when the times of the operators are comparable. Here we report the results of a preliminary investigation. Specifically, Fig. 9 shows the dynamical correlation functions

$$C(t \cos \varphi, t \sin \varphi) = \langle \sigma_j^x(t \cos \varphi) \sigma_\ell^x(t \sin \varphi) \rangle_{c,0}, \quad (62)$$

where sites  $j, n$  correspond to the same rescaled position, but at different times, i.e.,  $z_{j,t \cos \varphi} = z_{\ell,t \sin \varphi}$ . The extrapolation to  $t \rightarrow \infty$  is obtained with the same procedure used to test stability against localised perturbations, and the meaning of the error bars is the same as in Fig. 8. We show only the extrapolation of the real part of the correlation function, as the imaginary part is consistent with zero in the limit  $t \rightarrow \infty$ . Even if we have not worked out a theoretical prediction for the non-equal time correlations, our extrapolations suggest quite clearly that the dynamical correlation functions are nonzero for  $t \rightarrow \infty$  in the entire range of  $\varphi$  investigated. This shows that the breakdown of clustering is not only in the space direction.

The universality properties of the equal-time correlations made us conjecture that a similar result could hold true for non-equal time correlations, i.e., eq. (52). We have performed a preliminary check of this conjecture. In particular, Fig. 10 reports the ratio

$$R = \text{Re}(\langle O_j(t_1) O_\ell(t_2) \rangle_{c,0}) / \text{Re}(\langle \sigma_j^x(t_1) \sigma_\ell^x(t_2) \rangle_{c,0}), \quad (63)$$

with  $O_j = \sigma_j^x \sigma_{j+1}^z$ . Even in this case the extrapolation to  $t \rightarrow \infty$  agrees with the prediction  $\langle O \rangle_{\text{GS}}^2 / \langle \sigma^x \rangle_{\text{GS}}^2$ .

We point out, however, that only a theoretical prediction for the late-time behaviour of non-equal time correla-

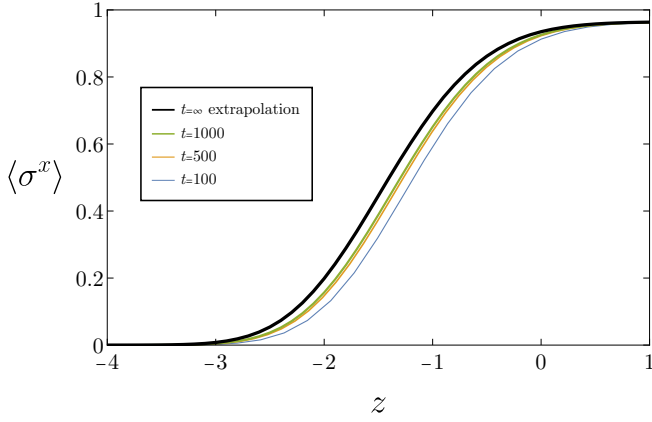


FIG. 11. The same as in Fig. 2 for  $\beta = 0$ .

tions could confirm or contradict these indications. Thus, we leave the behaviour of non-equal time correlations as an open question deserving further investigations.

#### D. Interfacial region width

Both our predictions and the numerical data that we exhibited point to the width of the interfacial region to grow as  $t^{1/3}$ . We discuss here the remaining dependence on the left reservoir, i.e., on  $\eta$ . We have shown in Fig. 2 the profile of the magnetization for different values of the temperature of the left reservoir. The plots suggest that the interfacial region becomes wider as the temperature is decreased. This is indeed the case, as shown in the following. We define the  $\epsilon$  rescaled width  $\xi_\epsilon$  of the interfacial region as the length of the interval of rescaled positions  $z$  for which  $\mathcal{M}_\eta(z)$  is in  $(\epsilon, 1 - \epsilon)$ . Note that, even if parameter  $\eta$  of the perturbative expansion diverges as  $\beta \rightarrow 0$ , the interfacial region does not shrink to zero in the limit of infinite temperature—see Fig. 11. In the low-temperature limit,  $\beta \rightarrow \infty$ , on the other hand, the rescaled width diverges, consistently with the findings of Ref. [13, 14, 34]. We estimate how  $\xi_\epsilon$  scales with  $\beta$  at fixed  $\epsilon$  by truncating the perturbation theory at first order,  $\mathcal{M}_\eta(z) = \exp(-\eta I_1(z))$ , indeed the first-order approximation becomes exact in the limit  $\beta \rightarrow \infty$  for given  $z$ , and it looks like it does it uniformly in  $z$ . Since  $\eta \sim 2 \exp[-2\beta\sqrt{1-h^2}]$  and  $I_1(z) \sim (-z)^{3/2}$  as  $z \rightarrow -\infty$  we conclude that the solution  $z_1$  of  $\mathcal{M}_\eta(z_1) = \epsilon$  scales as  $\exp[4\beta\sqrt{1-h^2}/3]$  as  $\beta \rightarrow \infty$ . On the other hand,  $I_1(z)$  approaches zero faster than any power as  $z \rightarrow \infty$ . Thus the right boundary of the interfacial region remains close to  $z = 0$  and is subleading with respect to  $-z_1$  as  $\beta \rightarrow \infty$ . From this it follows  $\xi_\epsilon \sim \exp[\frac{4}{3}\beta\sqrt{1-h^2}]$ . Note that the effective theory describing the edge of the lightcone does not capture the behaviour at a distance  $\sim t$  from the edge, hence, by consistency, this estimation makes sense only if time is so large that  $\xi_\epsilon \ll t^{2/3}$ .

## V. ENTANGLEMENT ASYMMETRY

Order parameters, such as the expectation values of nonsymmetric operators, are not the only tools to investigate symmetry breaking. An alternative/complementary quantity that has been recently introduced is the “entanglement asymmetry” [37]. The quantity has already received substantial attention [50–60]. Its most evident advantage is that it is only a property of the state of the (sub)system and of the symmetry group. As remarked in Ref. [50] in the context of global quenches in the transverse-field Ising model, the entanglement asymmetry witnesses symmetry breaking even when the standard order parameter vanishes.

The entanglement asymmetry is defined for a density matrix  $\rho_A$  and a finite symmetry group  $G$  acting on it as

$$\Delta S_A = S(\rho_{A,G}) - S(\rho_A), \quad (64)$$

where  $S(\rho) = -\text{tr}(\rho \log \rho)$  is the Von-Neumann entropy and  $\rho_{A,G}$  is the state of the subsystem after applying a random element of the symmetry group with equal probabilities. That is to say, if the group has a finite dimension  $|G|$ , we have

$$\rho_{A,G} = \frac{1}{|G|} \sum_{g \in G} g \rho_A g^{-1}. \quad (65)$$

En passant, note that this definition can be used for a generic subsystem  $A$  only if the group is generated by a local charge  $Q = \sum_i Q_i$  whose density  $Q_i$  has support on a single site; the action of an element  $g \in G$  is then well defined on  $\rho_A$ . The properties of the von Neumann entropy ensure that the asymmetry is positive, bounded by  $\log |G|$  and is zero if and only if  $g \rho_A g^{-1} = \rho_A$  for all  $g \in G$ . One can conclude that  $\rho_A$  is symmetric if and only if  $\Delta S_A$  is zero, whereas  $\rho_A$  completely breaks the symmetry if  $\Delta S_A = \log |G|$ . Just as the von Neumann entropy is often generalised to Rényi- $\alpha$  entropies,

$$S^{(\alpha)}(\rho) = \frac{1}{1-\alpha} \log(\text{tr}(\rho^\alpha)) \quad (66)$$

(the von Neumann entropy corresponds to the limit  $\alpha \rightarrow 1^+$ ), the asymmetry is naturally generalised to Rényi- $\alpha$  asymmetries  $\Delta S_A^{(\alpha)}$  by replacing the von-Neumann entropies with the Rényi- $\alpha$  ones in the definition (64).

The ferromagnetic ground state of the transverse-field Ising chain breaks the  $\mathbb{Z}_2$  symmetry corresponding to the group  $G = \{I, P\}$ , where  $I$  is the identity and  $P = \prod_j \sigma_j^z$  is the spin flip operator. Consequently,

$$\rho_{A,\mathbb{Z}_2} = \frac{1}{2} \rho_A + \frac{1}{2} P_A \rho_A P_A \quad (67)$$

where  $P_A = \prod_{j \in A} \sigma_j^z$ , which is the even part of the reduced density matrix  $\rho_A$ .

### A. Free-fermion technique

The  $\mathbb{Z}_2$  Rényi- $\alpha$  asymmetry shares, with the order parameter correlations, the complication of requiring to compute the expectation value of odd observables, i.e., observables that anticommute with the spin flip operator ( $OP = -PO$ ). Consider, for example, the Rényi-2 asymmetry. It is convenient to decompose the reduced density matrix  $\rho_A = \rho_{A,e} + \rho_{A,o}$  into an even part,  $\rho_{A,e}$ , and an odd part,  $\rho_{A,o}$ , in such a way that the former commutes with  $P_A$  and the latter anticommutes with it. Then we have

$$\Delta S_A^{(2)} = \log\left(1 + \frac{\text{tr}(\rho_{A,o}^2)}{\text{tr}(\rho_{A,e}^2)}\right), \quad (68)$$

where

$$\text{tr}(\rho_{A,o}^2) = \frac{1}{2^{|A|}} \sum_{O_{A,\text{odd}}} \langle O_A \rangle^2, \quad (69)$$

for a system of  $|A|$  spins. Here the sum is over odd involutions,  $O_A^2 = I$ . In principle, each term of the sum can be computed using cluster decomposition as we did for the order parameter. The number of odd observables to compute, however, grows exponentially with  $|A|$ , so this approach is not appropriate for large subsystems. Ref. [50] proposed a trick to circumvent this issue. The idea is to express the odd part of  $\rho_A$  as the product of a simple operator with a Gaussian. For example, for  $j \in A$  we have

$$\rho_{A,o} = \text{tr}(\sigma_j^x \rho_A) \sigma_j^x \tilde{\rho}_A \quad (70)$$

where  $\tilde{\rho}_A$  is the normalised Gaussian

$$\tilde{\rho}_A = \lim_{r \rightarrow \infty} \frac{\text{tr}_B(\sigma_j^x \sigma_r^x \rho_e)}{\text{tr}(\sigma_j^x \sigma_r^x \rho_e)}. \quad (71)$$

Its correlation matrix  $\tilde{\Gamma}_A$  can be computed using Pfaffians (or a Schur complement, which can make the calculation faster [50]). Let us then define matrices  $\Gamma_{A,0}$  and  $\Gamma_{A,1}$  with elements  $(\Gamma_{A,0})_{ij} = \Gamma_{ij}$  and  $(\Gamma_{A,1})_{ij} = \tilde{\Gamma}_{ij}$  with  $i, j \in A$ . It turns out that the Rényi- $n$  entanglement asymmetry can be expressed as follows

$$\Delta S_A^{(n)} = \frac{1}{n-1} \log \left[ \sum_{\vec{\chi}} c_{\vec{\chi}} \frac{\{\Sigma_1^{s_1} \Gamma_{A,\chi_1} \Sigma_1^{s_1}, \dots, \Sigma_1^{s_n} \Gamma_{A,\chi_n} \Sigma_1^{s_n}\}}{\{\Gamma_{A,0}, \dots, \Gamma_{A,0}\}} \right], \quad (72)$$

where the sum is over  $\vec{\chi} = (\chi_1, \dots, \chi_n)$  with  $\chi_j \in \{0, 1\}$ ,  $s_l = \sum_{j=1}^l \chi_j$  and  $c_{\vec{\chi}} = \frac{1+(-1)^{s_n}}{2} \langle \sigma_1^x \rangle^{s_n}$ . In (72) we are using the bracket notations of Ref. [61], according to which the trace of the product of  $n$  Gaussian density matrices  $\rho_1, \dots, \rho_n$  with correlation matrices  $\Gamma_1, \dots, \Gamma_n$  reads  $\text{tr}(\rho_1 \dots \rho_n) = \{\Gamma_1, \dots, \Gamma_n\}$ . Such products can be defined recursively as follows [61]

$$\{\Gamma_1, \dots, \Gamma_n\} = \{\Gamma_1, \Gamma_2\} \{\Gamma_1 \times \Gamma_2, \Gamma_3, \dots, \Gamma_n\}, \quad (73)$$

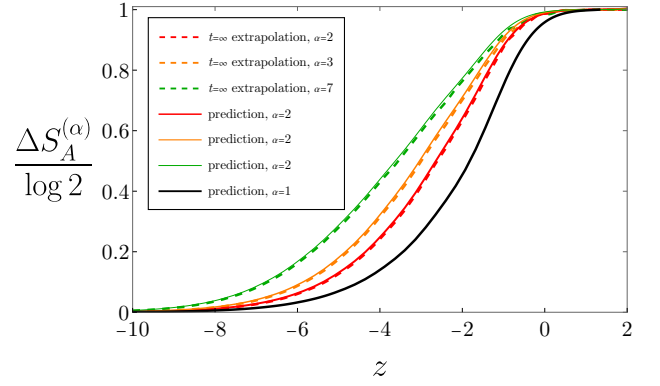


FIG. 12. Rényi- $\alpha$  and Von-Neumann ( $\alpha = 1$ ) asymmetries of a comoving subsystem  $A$  whose left and right boundaries have rescaled coordinates  $-12$  and  $z$ . The dotted lines correspond to the  $t \rightarrow \infty$  limit obtained by extrapolation of the numerical data, while the plain lines correspond to prediction (77).

where  $\Gamma_1 \times \Gamma_2$  stands for the correlation matrix of the normalised product of two Gaussians with correlation matrices  $\Gamma_1$  and  $\Gamma_2$  and is given by

$$\Gamma_1 \times \Gamma_2 = I - (I - \Gamma_2) \frac{I}{I + \Gamma_1 \Gamma_2} (I - \Gamma_1); \quad (74)$$

$\{\Gamma_1, \Gamma_2\}$  is the product of the eigenvalues of  $\frac{I + \Gamma_1 \Gamma_2}{2}$  with halved degeneracy (each eigenvalue is doubly degenerate because the correlation matrices are skew symmetric):

$$\{\Gamma_1, \Gamma_2\} = \prod_{\mu \in \text{spec}(\Gamma_1 \Gamma_2)/2} \frac{1+\mu}{2}. \quad (75)$$

Representation (72) is appropriate to compute the Rényi- $n$  asymmetry for small enough integer  $n > 1$ . We are not aware of an analogous free-fermion representation of the von Neumann asymmetry.

### B. Conjecture and numerical checks

For systems that satisfy  $|A| \ll t^{1/3}$ , it is straightforward to derive an analytical formula for the Rényi- $\alpha$  and von Neumann asymmetry using that the expectation value of every local even observable approaches the ground state value, while the expectation value of every odd observable is multiplied by the scaling function  $\mathcal{M}_\eta(z)$ . This implies that the reduced density matrix of subsystem  $A$  is

$$\rho_A = \frac{1 + \mathcal{M}_\eta(z)}{2} \rho_A^{\text{GS}} + \frac{1 - \mathcal{M}_\eta(z)}{2} P_A \rho_A^{\text{GS}} P_A, \quad (76)$$

where  $\rho_A^{\text{GS}}$  is the corresponding reduced density matrix in the ground state. Since there is no string order associated with the aforementioned spin-flip symmetry in the ferromagnetic ground state, for large enough subsystems (such that  $\log 2 - \Delta S_A \ll 1$ ),  $\|\rho_A^{\text{GS}} P_A \rho_A^{\text{GS}}\|$  is exponentially smaller than  $\|\rho_A^{\text{GS}} \rho_A^{\text{GS}}\|$ , hence we get

$$\Delta S_A^{(\alpha)} = \log 2 - H_\alpha(\mathcal{M}_\eta(z)) + o(|A|^{-\gamma}) \quad (77)$$



as  $|A| \rightarrow \infty$ , for any  $\gamma > 0$ , where  $H_\alpha(x)$  is the Rényi- $\alpha$  entropy function of a single bit of information

$$H_\alpha(x) = \frac{1}{1-\alpha} \log \left( \left( \frac{1+x}{2} \right)^\alpha + \left( \frac{1-x}{2} \right)^\alpha \right). \quad (78)$$

This is expected to remain true also in the limit  $\alpha \rightarrow 1^+$ , in which  $H_\alpha$  approaches the Shannon entropy function  $H_1(x) = -\frac{1+x}{2} \log \frac{1+x}{2} - \frac{1-x}{2} \log \frac{1-x}{2}$ .

It is reasonable to expect that, subleading corrections apart, the asymptotic result (77) captures also the late time behaviour of a subsystem  $A$ —in the right edge comoving frame—with boundaries at rescaled positions  $(z_l, z)$  intersecting the interfacial region. An argument supporting this conclusion follows. The starting point is to assume that (77) is correct when  $z_l$  approaches  $z$ . Let us then identify the effect of moving the left boundary  $z_l$  to the left. First we observe that  $P_A \rho_A^{\text{GS}} P_A$  corresponds to the contribution coming from having an odd number of excitations to the right hand side of  $A$ : The string operator  $P$ , indeed, maps one symmetry breaking ground state into the other, which is what a quasilocalised (semilocal) excitation does to the left hand side of its position. This is quantitatively captured by the scaling function at the right boundary of the subsystem, independently of how large the subsystem is. Thus, we argue that  $\rho_A$  keeps the same structure as in (77), provided to replace  $\rho_A^{\text{GS}}$  with the appropriate density matrix. Since we still do not expect string order in the state, we end up with (77) even when  $z - z_l$  does not approach 0.

We have checked this conjecture considering semi-infinite subsystems—in the right edge comoving frame—with the right boundary at given rescaled position. Fig. 12 shows a comparison between conjecture (77) and numerical data. The extrapolation to  $t \rightarrow \infty$  is obtained assuming  $\sim t^{-1/3}$  and  $\sim t^{-2/3}$  corrections and perfectly agrees with the prediction (the tiny but visible discrepancy can be traced back to the truncation of the perturbative expansion used to approximate the scaling function).

We remark that the strong link between the asymptotic behaviour captured by (77) and the asymptotics of the order parameter (6) is generally absent after global quenches, where, instead, the  $\mathbb{Z}_2$  entanglement asymmetry of a subsystem can be order 1 while the local longitudinal magnetization approaches zero [50].

## VI. WIGNER-YANASE SKEW INFORMATION

The protocol that we studied is special since, generally, the size of fully correlated clusters remains finite even at late times when time evolving under translationally invariant Hamiltonians with local interactions. In the interfacial region, on the other hand, we have shown that such size diverges as  $t^{1/3}$ . We are aware of other one-dimensional settings in which similar exceptional properties are triggered by localized or semi-localized perturbations:

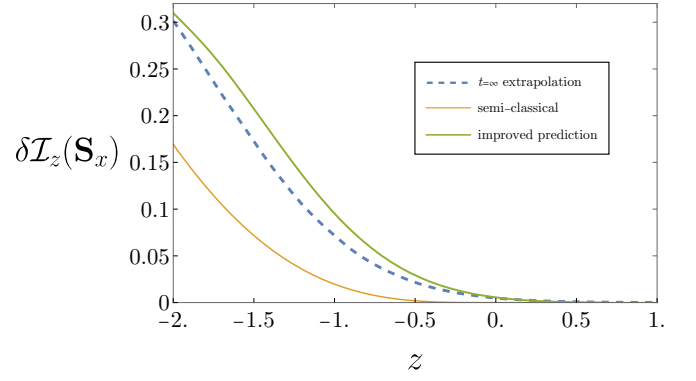


FIG. 13. Skew information profile for the semi-infinite subsystem with  $\beta = 0$ .

- in symmetry breaking ground states [13, 15, 17, 33].
- in symmetric states in the presence of semilocal conservation laws [62].
- in jammed states of kinetically constrained systems [63–65].
- in separable—or, with both low bipartite and low multipartite entanglement—quantum scars [66].

Refs [17, 65, 66], in particular, point out that the corresponding clusters are not only full-range classically correlated, but also full-range quantum correlated.

We find it reasonable to identify the quantum part of the variance of an operator  $O$  with a quarter of the quantum Fisher information  $F_\rho(O)$ , indeed Refs [67, 68] showed that  $\frac{1}{4}F_\rho(O)$  is the convex roof of the variance

$$\frac{1}{4}F_\rho(O) = \inf_{\{p_i, |\Psi_i\rangle\}} \sum_i p_i [\langle \Psi_i | O^2 | \Psi_i \rangle - \langle \Psi_i | O | \Psi_i \rangle^2] \quad (79)$$

where the infimum is taken over all possible convex decompositions of the density matrix,  $\rho$ , in pure states,  $\rho = \sum_i p_i |\Psi_i\rangle \langle \Psi_i|$ . We remark that Ref. [39] proposed an alternative definition

$$\Delta_Q^2 O = -\frac{1}{2} \int_0^1 d\alpha \text{tr}([O, \rho^\alpha][O, \rho^{1-\alpha}]), \quad (80)$$

but there are constants  $\kappa_{1,2}$  such that  $\kappa_1 \Delta_Q^2 O \leq \frac{1}{4}F_\rho(O) \leq \kappa_2 \Delta_Q^2 O$ , hence the two definitions are equivalent. Since we are not aware of an efficient way to compute the quantum Fisher information in a subsystem of an almost Gaussian state, such as the one under investigation, we have opted for computing an equivalent—in the same sense as before—quantity: the Wigner-Yanase skew information

$$I_\rho(O) = -\frac{1}{2} \text{tr}([O, \rho^{1/2}]^2). \quad (81)$$

Since we already showed that the two-point function of  $\sigma^x$  does not cluster in the interfacial region, we consider



$I_{\rho_A}(S_A^x)$  in subsystems  $A$  in the right edge comoving frame. This quantity can be computed in a Gaussian state with free fermion techniques, as follows. The first step is to express the skew information as

$$I_{\rho_A}(S_A^x) = \frac{1}{4} \sum_{\ell, n \in A} \text{tr} \left( (\rho_A - \kappa_A^{(\ell)} \tilde{\rho}_A^{(\ell)}) \sigma_\ell^x \sigma_n^x \right) \quad (82)$$

where  $\kappa_A^{(\ell)}$  equals  $\text{tr}(\rho_A^{1/2} \sigma_\ell^x \rho_A^{1/2} \sigma_\ell^x)$  and  $\tilde{\rho}_A^{(\ell)}$  is the normalised Gaussian

$$\tilde{\rho}_A^{(\ell)} = (\kappa_A^{(\ell)})^{-1} \rho_A^{1/2} \sigma_\ell^x \rho_A^{1/2} \sigma_\ell^x. \quad (83)$$

Both  $\kappa_A^{(\ell)}$  and the correlation matrix of  $\tilde{\rho}_A^{(\ell)}$  can be easily expressed in terms of the correlation matrix  $\Gamma_A$  of  $\rho_A$  within the formalism developed in Ref. [61]. Specifically, if  $\Sigma_{(2\ell-1)}$  is the diagonal involution with the first  $2\ell-1$  diagonal elements equal  $-1$  and the rest of them equal  $1$ , we have

$$\kappa_A^{(\ell)} = \sqrt{\det \left[ \left( I + \left( \frac{1 - \sqrt{1 - \Gamma_A^2}}{\Gamma_A} \Sigma_{(2\ell-1)} \right)^2 \right) / 2 \right]} \quad (84)$$

and

$$\tilde{\Gamma}_A^{(\ell)} = \frac{1 - \sqrt{1 - \Gamma_A^2}}{\Gamma_A} \times \left( \Sigma_{(2\ell-1)} \frac{1 - \sqrt{1 - \Gamma_A^2}}{\Gamma_A} \Sigma_{(2\ell-1)} \right), \quad (85)$$

where  $\Gamma_1 \times \Gamma_2$  was defined in (74). We are then left with a sum of expectation values of  $\sigma_\ell^x \sigma_n^x$  in Gaussian states, as in eq. (40).

To highlight the breakdown of clustering in the interfacial region, we study the increase of W-Y skew information  $\Delta I_z[S^x]$  in half-infinite subsystems in the edge comoving frame with the left boundary within the interfacial region:  $A_t(z) = \{j, j+1, j+2, \dots\}$  where  $z_{j-1,t} < z < z_{j,t}$

$$\Delta I_z(S^x) = I_{\rho_{A_t(z)}(t)}(S_{A_t(z)}^x) - I_{\rho_{A_t(z)}(0)}(S_{A_t(z)}^x). \quad (86)$$

This is finite by virtue of the Lieb-Robinson bounds as the contribution from the operators sufficiently far to the right from the edge of the lightcone cancels with the corresponding one at the initial time. Thus,  $A_t(z)$  could be replaced by a subsystem that extends from rescaled position  $z$  to a positive rescaled position  $z_{\max} \sim 1$  without affecting the result. The effective size of the latter subsystem is  $\sim t^{1/3}$ . In view of this, we compute  $\delta \mathcal{I}_z(S^x) \equiv |v''(\bar{p})t|^{-2/3} \Delta I_z(S^x)$ , which can approach a nonzero value in the limit  $t \rightarrow \infty$  only if quantum correlations do not cluster within the interfacial region. An example is reported in Fig. 13, in which we show the  $z$  dependence of an extrapolation to  $t \rightarrow \infty$ . It is evident that  $\delta \mathcal{I}_z(S^x)$  remains nonzero for values of  $z$  in the interfacial region, proving that the region is full-range quantum correlated.

## VII. PHYSICAL INTERPRETATION

We propose here a basic semiclassical description that provides a good approximation for the order parameter correlations and a fair one for the Wigner-Yanase skew information. Since around the edge we are close to zero temperature, as a starting point we take the semiclassical theory developed by Sachdev and Young in Ref. [69]. The excitations are then described by classical particles traveling at constant speed. Odd operators are semilocal with respect to the elementary excitations, that is to say, their expectation values change sign when a particle crosses their position. This results in the following semiclassical representation for the one-point function of a local odd operator  $O(z)$  at rescaled position  $z$

$$\langle O(z) \rangle \stackrel{\text{s.c.}}{=} \langle O(z) \rangle_{\text{GS}} \sum_j (-1)^j P(\mathcal{A}_j^{(z, \infty)}), \quad (87)$$

where  $P(\mathcal{A}_j^{(z_1, z_2)})$  stands for the probability that there are  $j$  particles in the (mobile) subsystem in the right edge comoving frame within rescaled positions  $z_1$  and  $z_2$ . (Here and in the following the probabilities are defined for a fixed large time  $t$ .) Analogously, the two-point function is represented as

$$\langle O(z_1) O(z_2) \rangle \stackrel{\text{s.c.}}{=} \langle O(z_1) O(z_2) \rangle_{\text{GS}} \sum_j (-1)^j P(\mathcal{A}_j^{(z_1, z_2)}). \quad (88)$$

We now compute such probabilities treating the excitations as classical particles. Since only the fastest particles can reach the interfacial region, it is convenient to rewrite the trajectory of the particles in rescaled coordinates:  $z = z_0 - \frac{1}{2}q^2$ , where we introduced a space variable,  $z_0 = \frac{x_0}{|v''(\bar{p})t|^{1/3}}$ , which becomes continuous in the limit of infinite time, and  $x_0$  labels the chain site where the particle was originated. Since the initial state has a finite correlation length, we can assume that, at large enough time, particles originated at different  $z_0$  are completely uncorrelated. Note that a fixed tiny interval  $\Delta z_0$  can be the origin of a number of particles that scales as  $t^{1/3}$ . Such particles are uncorrelated as long as their distance is larger enough than the local correlation length in the initial state. We shall make the approximation that there are no correlations between the classical particles at the initial time, which can be rephrased as that only one particle can be originated in the infinitesimal interval  $(z_0, z_0 + dz_0)$ . The probability to have one excitation with a finite rescaled momentum  $q$  at  $z_0$  at the initial time is asymptotically independent of  $q$  and given by

$$P((z_0, z_0 + dz_0) \mathcal{A}_{(q, q+dq)}) = \frac{1 - e^{-\eta}}{4\pi} \theta_H(-z_0) dz_0 dq \quad (89)$$

A particle originated at  $z_0$  has crossed  $z$  before time  $t$  only if its rescaled momentum  $q$  is smaller than  $\sqrt{2(z_0 - z)}$  in absolute value, therefore the joined probability that a

particle was produced at  $z_0$  and, at time  $t$ , is to the right hand side of rescaled position  $z$  reads

$$P((z_0, z_0+dz_0) \nearrow^{(z, \infty)}) = \frac{1-e^{-\eta}}{\sqrt{2\pi}} \sqrt{z_0 - z} \theta_H(z_0 - z) dz_0. \quad (90)$$

Since particles are assumed to be uncorrelated, this directly gives the probability to have 0 particles to the right hand side of rescaled position  $z$

$$\begin{aligned} P(\mathcal{A}_0^{(z, \infty)}) &= e^{-\int_{-\infty}^0 P((z_0, z_0+dz_0) \nearrow^{(z, \infty)})} \\ &= e^{-\frac{\sqrt{2}(1-e^{-\eta})}{3\pi} (-z)^{\frac{3}{2}} \theta_H(-z)}. \end{aligned} \quad (91)$$

Note that for  $z \geq 0$  the probability is estimated to become exactly 1 because the maximal velocity is a hard upper bound for classical particles. Analogously we have

$$\begin{aligned} P(\mathcal{A}_j^{(z, \infty)}) &= \frac{[\int_{-\infty}^0 P((z_0, z_0+dz_0) \nearrow^{(z, \infty)})]^j}{j!} e^{-\int_{-\infty}^0 P((z_0, z_0+dz_0) \nearrow^{(z, \infty)})} \\ &= \frac{[\frac{\sqrt{2}(1-e^{-\eta})}{3\pi} (-z)^{\frac{3}{2}}]^j}{j!} e^{-\frac{\sqrt{2}(1-e^{-\eta})}{3\pi} (-z)^{\frac{3}{2}}}. \end{aligned} \quad (92)$$

The semiclassical approximation of the one-point function, and, in turn, of the one-point scaling function is then readily obtained—cf. (87) and (92)

$$\mathcal{M}_\eta(z) \stackrel{\text{s.c.}}{=} P(\mathcal{A}_0^{(z, \infty)})^2 = e^{-\frac{2\sqrt{2}(1-e^{-\eta})}{3\pi} (-z)^{\frac{3}{2}}}. \quad (93)$$

By repeating the same steps for the 2-point function—eq. (88)—we find

$$\begin{aligned} \mathcal{M}_\eta(z_1, z_2) &\stackrel{\text{s.c.}}{=} \frac{P(\mathcal{A}_0^{(z_1, \infty)})^2}{P(\mathcal{A}_0^{(z_2, \infty)})^2} \\ &= e^{-\frac{2\sqrt{2}(1-e^{-\eta})}{3\pi} [(-z_1)^{\frac{3}{2}} - (-z_2)^{\frac{3}{2}}]}. \end{aligned} \quad (94)$$

We are also in the position to estimate the variance per unit  $|v''(\bar{p})t|^{2/3}$  of an extensive odd operator in a subsystem in the right edge comoving frame characterised by  $(z_1, z_2)$ :

$$\begin{aligned} \lim_{t \rightarrow \infty} \frac{1}{|v''(\bar{p})t|^{2/3} \langle O \rangle_{\text{GS}}^2} \langle \sum_{z_\ell, t \in (z_1, z_2)} O_\ell, \sum_{z_\ell, t \in (z_1, z_2)} O_\ell \rangle_c \\ \stackrel{\text{s.c.}}{\approx} 4 \int_{z_1}^{z_2} dz'_1 e^{-\frac{2\sqrt{2}(1-e^{-\eta})}{3\pi} (-z'_1)^{\frac{3}{2}}} \\ \int_{z'_1}^{z_2} dz'_2 \sinh\left(\frac{2\sqrt{2}(1-e^{-\eta})}{3\pi} (-z'_2)^{\frac{3}{2}}\right) \\ \sim \frac{16\sqrt{2}(1-e^{-\eta})}{105\pi} [2(-z_1)^{\frac{7}{2}} + 7z_1(-z_2)^{\frac{5}{2}} + 5(-z_2)^{\frac{7}{2}}] \end{aligned} \quad (95)$$

for  $z_1 < z_2 \leq 0$ ; the result for  $z_2$  larger than 0 is obtained by replacing  $z_2$  with 0. Notwithstanding the simplicity of the derivation, these semiclassical approximations are rather good for small  $\eta$  and they also capture the leading asymptotic behaviour of  $I_1(z)$  for large  $(-z)$ .

While the physical interpretation that we provided is essentially classical, we can use it also to estimate the Wigner-Yanase skew information, which captures purely

quantum correlations. At first sight, this might sound impossible; the secret to get a nonzero result is to complement the semiclassical description by additional information, which is beyond the classical theory. Specifically, for a half-infinite subsystem in the edge comoving frame with the left boundary at rescaled position  $z$  close to the edge of the lightcone, we found the following assumptions to be consistent with the numerical observations.

- The contributions coming from more than one particle in the subsystem are negligible.
- The single particle sector associated with a particle originated at a given  $z_0$  is quantum coherent.
- Contributions from particles originated at different  $z_0$  are incoherent, and that is the only source of incoherence.

Under these assumptions, the Wigner-Yanase skew information equals a quarter of the quantum Fisher information and can be expressed in terms of the classical probabilities as follows

$$\begin{aligned} \frac{I_z[\sum_{z_\ell, t \in (z, \infty)} O_\ell]}{|v''(\bar{p})t|^{2/3} \langle O \rangle_{\text{GS}}^2} \\ \stackrel{\text{s.c.}}{=} 8 \int_{-\infty}^0 P(\mathcal{A}_1^{(z, \infty)}, (z_0, z_0+dz_0) \nearrow^{(z, \infty)}) \\ \int_z^\infty dz_1 \int_{z_1}^\infty dz_2 \frac{P((z_0, z_0+dz_0) \nearrow^{(z_2, \infty)})}{P((z_0, z_0+dz_0) \nearrow^{(z, \infty)})} \\ \left(1 - \frac{P((z_0, z_0+dz_0) \nearrow^{(z_1, \infty)})}{P((z_0, z_0+dz_0) \nearrow^{(z, \infty)})}\right). \end{aligned} \quad (96)$$

Here  $P(\mathcal{A}_1^{(z, \infty)}, (z_0, z_0+dz_0) \nearrow^{(z, \infty)})$  stands for the probability that there is only one particle in the subsystem and that that particle was originated in  $(z_0, z_0+dz)$ . The rest of the expression comes from expressing the variance in terms of probabilities as done above under the condition that the unique particle that is present in the subsystem was originated at  $z_0$  [70].

Within the semiclassical picture we have

$$\begin{aligned} P(\mathcal{A}_1^{(z, \infty)}, (z_0, z_0+dz_0) \nearrow^{(z_1, z_2)}) \\ = \frac{1-e^{-\eta}}{\sqrt{2\pi}} [(z_0 - z_1)^{\frac{1}{2}} - (z_0 - z_2)^{\frac{1}{2}}] e^{-\frac{\sqrt{2}(1-e^{-\eta})}{3\pi} (-z)^{\frac{3}{2}}} dz_0. \end{aligned} \quad (97)$$

Thus, the probability that the particle originated at  $z_0$  is in  $(z_1, z_2)$  given that there's a single particle to the right hand side of  $z$  is

$$\frac{P(\mathcal{A}_1^{(z, \infty)}, (z_0, z_0+dz_0) \nearrow^{(z_1, z_2)})}{P(\mathcal{A}_1^{(z, \infty)})} = \left[ \left( \frac{z_0 - z_1}{z_0 - z} \right)^{\frac{1}{2}} - \left( \frac{z_0 - z_2}{z_0 - z} \right)^{\frac{1}{2}} \right] dz_0 \quad (98)$$

We can then express the contribution to the one- and two-point function of  $O$  restricted to particles originated at  $z_0$  and knowing that there's only one particle in the

subsystem as follows

$$\frac{\langle O(z) \rangle^{(z_0)}}{\langle O \rangle_{\text{GS}}} = 1 - 2 \left( \frac{z_0 - z}{z_0 - z} \right)^{\frac{1}{2}} \quad (99)$$

$$\frac{\langle O(z_1) O(z_2) \rangle^{(z_0)}}{\langle O \rangle_{\text{GS}}^2} = 1 - 2 \left( \frac{z_0 - z_1}{z_0 - z} \right)^{\frac{1}{2}} + 2 \left( \frac{z_0 - z_2}{z_0 - z} \right)^{\frac{1}{2}} \quad (100)$$

The corresponding variance per unit  $|v''(\bar{p})t|^{2/3}$  equals  $\frac{16}{45}(z_0 - z)^2 \langle O \rangle_{\text{GS}}^2$ , and hence the Wigner-Yanase skew information is estimated as follows

$$\frac{I_z[\sum_{z_\ell, t \in (z, \infty)} O_\ell]}{|v''(\bar{p})t|^{2/3} \langle O \rangle_{\text{GS}}^2} \stackrel{\text{s.c.}}{=} \frac{32}{315} \frac{1 - e^{-\eta}}{\sqrt{2\pi}} (-z)^{\frac{7}{2}} e^{-\frac{\sqrt{2}(1 - e^{-\eta})}{3\pi}} (-z)^{\frac{3}{2}} \quad (101)$$

The comparison with numerical data for not too large  $-z$  is qualitatively fair but quantitatively poor—cf. Fig. 13. One of the reasons behind it is that the semiclassical approximation for the probabilities is already leaving out quantum contributions that are of the same order as the contributions considered here. To some extent, we can reintroduce them by hand. Specifically, we propose to identify the probability to have zero particles in a subsystem (in the right edge comoving frame)  $P(\mathcal{Z}_0^{(z_1, z_2)})$  with the overlap between the reduced density matrix and the corresponding one in the initial state. The calculation follows the same steps as for the order parameter correlation, and indeed the result is very similar:

$$P(\mathcal{Z}_0^{(z_1, z_2)}) = \mathcal{M}_{\tilde{\eta}}(z_1, z_2), \quad P(\mathcal{Z}_0^{(z, \infty)}) = \mathcal{M}_{\tilde{\eta}}(z_1), \quad (102)$$

with  $\tilde{\eta} = \log \frac{2}{1 + e^{-\eta}}$ . We keep the same assumptions as in the semiclassical approximation; for example, we have

$$\begin{aligned} P((z_0, z_0 + dz_0) \nearrow^{(z, \infty)}) &= -\partial_{z_0} \log \left( P(\mathcal{Z}_0^{(z - z_0, \infty)}) \right) dz_0 \\ &= -\partial_{z_0} \log (\mathcal{M}_{\tilde{\eta}}(z - z_0)) dz_0. \end{aligned} \quad (103)$$

The result at the leading order of the perturbation theory according to which  $\mathcal{M}_{\tilde{\eta}}(z) \sim e^{-\tilde{\eta} I_1(z)}$  is the following refined approximation

$$\begin{aligned} \frac{I_z[\sum_{z_\ell, t \in (z, \infty)} O_\ell]}{|v''(\bar{p})t|^{2/3} \langle O \rangle_{\text{GS}}^2} &\sim \\ 4\tilde{\eta} e^{-\tilde{\eta} I_1(z)} \int_z^\infty dz_0 &\left[ \frac{[I_1(z_0)]^2}{I_1'(z_0)} + 2 \int_{z_0}^\infty dz' I_1(z') \right]. \end{aligned} \quad (104)$$

which is the formula that we compared against numerical data in Ref. [16]. The reader can appreciate how much this refined prediction outperforms the semiclassical approximation by revisiting Fig. 13. As a final note, we disclose that, within the interval of rescaled positions shown in the figure, the residual discrepancy between prediction and extrapolation arises almost entirely from the error coming from approximating the probability of having zero particles to the right of the rescaled position  $z$  by  $e^{-\tilde{\eta} I_1(z)}$ .

## VIII. CONCLUSIONS

In this work we have derived analytic expressions for the time evolution of one- and two-point functions in the transverse field Ising chain after joining a symmetry breaking ground state with a disordered state. We identified an interfacial region near the right edge of the light cone, scaling as  $t^{1/3}$ , where correlations converge to universal functions. Within this region, we demonstrated that correlations are full-range, and we computed the Wigner-Yanase skew information of the order parameter to confirm that these strong correlations include a quantum component. We have studied the entanglement asymmetry of subsystems within the interfacial region and obtained an analytic prediction that exhibits the same degree of universality as the order parameter correlation functions. We have proposed a semiclassical theory based on the Sachdev-Young one, which helps one understand the behaviour of correlations, asymmetry, and even quantum Fisher information in the interfacial region.

In light of the exceptional classical and quantum properties near the edge of the lightcone that we pointed out, we think that it is compelling to supplement our investigation with the study of other quantities, such as the entanglement negativity [71–78], the mutual and the tripartite information [79–84] (we are particularly curious about the residual value of the latter [85–88]), the Markov gap [89, 90], and the entanglement Hamiltonian [91–93].

In Ref. [16] we argued that the phenomenology that we unveiled extends to interacting integrable systems, but a detailed analysis is still lacking, and it is unclear what to expect in the presence of integrability breaking interactions. To shed light on interacting integrable systems, it might be of interest to obtain some of the results of this work within a form factor approach [94, 95]. And in view of the universality of the behaviours, we think that it could be instructive to derive the results again within the framework of a quantum field theory [34]. In more generic systems, numerical methods based on tensor networks could help recognize the crucial properties of the interfacial region. In that respect, we wonder whether some aspects could also be addressed through quantum circuits. While we have considered time evolution in an isolated system, the protocol that we studied has a direct analogue in open quantum systems [96], where one could imagine to prepare a semi-infinite system in a symmetry breaking ground state and put it in contact with a disordered reservoir at the boundary described by a Lindblad master equation. Finally, in light of recent advances in quantum quenches [97, 98] and interface dynamics [99–101] in higher dimensions, we wonder whether the problem of joining an ordered state with a disordered reservoir could be effectively addressed also in two and three dimensions.

## ACKNOWLEDGMENTS

This work was supported by the European Research Council under the Starting Grant No. 805252 LoCo-Macro.

- 
- [1] A. Polkovnikov, K. Sengupta, A. Silva, and M. Vengalattore, Colloquium: Nonequilibrium dynamics of closed interacting quantum systems, *Rev. Mod. Phys.* **83**, 863 (2011).
  - [2] C. Gogolin and J. Eisert, Equilibration, thermalisation, and the emergence of statistical mechanics in closed quantum systems, *Rep. Prog. Phys.* **79**, 056001 (2016).
  - [3] O. A. Castro-Alvaredo, B. Doyon, and T. Yoshimura, Emergent Hydrodynamics in Integrable Quantum Systems Out of Equilibrium, *Phys. Rev. X* **6**, 041065 (2016).
  - [4] B. Bertini, M. Collura, J. De Nardis, and M. Fagotti, Transport in Out-of-Equilibrium  $XXZ$  Chains: Exact Profiles of Charges and Currents, *Phys. Rev. Lett.* **117**, 207201 (2016).
  - [5] M. Borsi, B. Pozsgay, and L. Pristiyák, Current operators in bethe ansatz and generalized hydrodynamics: An exact quantum-classical correspondence, *Phys. Rev. X* **10**, 011054 (2020).
  - [6] V. Alba, B. Bertini, M. Fagotti, L. Piroli, and P. Ruggiero, Generalized-hydrodynamic approach to inhomogeneous quenches: correlations, entanglement and quantum effects, *Journal of Statistical Mechanics: Theory and Experiment* **2021**, 114004 (2021).
  - [7] J. D. Nardis, B. Doyon, M. Medenjak, and M. Panfil, Correlation functions and transport coefficients in generalised hydrodynamics, *Journal of Statistical Mechanics: Theory and Experiment* **2022**, 014002 (2022).
  - [8] V. B. Bulchandani, S. Gopalakrishnan, and E. Ilievski, Superdiffusion in spin chains, *Journal of Statistical Mechanics: Theory and Experiment* **2021**, 084001 (2021).
  - [9] M. Borsi, B. Pozsgay, and L. Pristiyák, Current operators in integrable models: a review, *Journal of Statistical Mechanics: Theory and Experiment* **2021**, 094001 (2021).
  - [10] F. H. Essler, A short introduction to Generalized Hydrodynamics, *Physica A: Statistical Mechanics and its Applications* **631**, 127572 (2023), lecture Notes of the 15th International Summer School of Fundamental Problems in Statistical Physics.
  - [11] E. Ilievski, E. Quinn, J. D. Nardis, and M. Brockmann, String-charge duality in integrable lattice models, *Journal of Statistical Mechanics: Theory and Experiment* **2016**, 063101 (2016).
  - [12] L. Piroli, J. De Nardis, M. Collura, B. Bertini, and M. Fagotti, Transport in out-of-equilibrium  $XXZ$  chains: Nonballistic behavior and correlation functions, *Phys. Rev. B* **96**, 115124 (2017).
  - [13] V. Eisler, F. Maislinger, and H. G. Evertz, Universal front propagation in the quantum Ising chain with domain-wall initial states, *SciPost Phys.* **1**, 014 (2016).
  - [14] V. Eisler and F. Maislinger, Front dynamics in the XY chain after local excitations, *SciPost Phys.* **8**, 37 (2020).
  - [15] V. Eisler and F. Maislinger, Hydrodynamical phase transition for domain-wall melting in the XY chain, *Phys. Rev. B* **98**, 161117 (2018).
  - [16] V. Marić, F. Ferro, and M. Fagotti, Macroscopic Quantum States and Universal Correlations in a Disorder-Order Interface Propagating over a 1D Ground State, *arXiv:2410.10645 [cond-mat.stat-mech]* (2024).
  - [17] F. Ferro and M. Fagotti (In preparation).
  - [18] S. Sachdev, *Quantum Phase Transitions*, 2nd ed. (Cambridge University Press, 2011).
  - [19] W. H. Aschbacher and C.-A. Pillet, Non-Equilibrium Steady States of the XY Chain, *Journal of Statistical Physics* **112**, 1153 (2003).
  - [20] T. Platini and D. Karevski, Scaling and front dynamics in Ising quantum chains, *The European Physical Journal B - Condensed Matter and Complex Systems* **48**, 225 (2005).
  - [21] C. A. Tracy and H. Widom, Level-spacing distributions and the Airy kernel, *Physics Letters B* **305**, 115 (1993).
  - [22] V. Hunyadi, Z. Rácz, and L. Sasvári, Dynamic scaling of fronts in the quantum  $XX$  chain, *Phys. Rev. E* **69**, 066103 (2004).
  - [23] V. Eisler and Z. Rácz, Full Counting Statistics in a Propagating Quantum Front and Random Matrix Spectra, *Phys. Rev. Lett.* **110**, 060602 (2013).
  - [24] G. Peretto and A. Gambassi, Ballistic front dynamics after joining two semi-infinite quantum ising chains, *Phys. Rev. E* **96**, 012138 (2017).
  - [25] M. Fagotti, Higher-order generalized hydrodynamics in one dimension: The noninteracting test, *Phys. Rev. B* **96**, 220302 (2017).
  - [26] D. Bernard and B. Doyon, Energy flow in non-equilibrium conformal field theory, *Journal of Physics A: Mathematical and Theoretical* **45**, 362001 (2012).
  - [27] A. De Luca, J. Viti, D. Bernard, and B. Doyon, Nonequilibrium thermal transport in the quantum ising chain, *Phys. Rev. B* **88**, 134301 (2013).
  - [28] G. Peretto and A. Gambassi, Dynamics of large deviations in the hydrodynamic limit: Noninteracting systems, *Phys. Rev. E* **102**, 042128 (2020).
  - [29] M. Kormos, Inhomogeneous quenches in the transverse field Ising chain: scaling and front dynamics, *SciPost Phys.* **3**, 020 (2017).
  - [30] M. Fagotti, Locally quasi-stationary states in noninteracting spin chains, *SciPost Phys.* **8**, 48 (2020).
  - [31] B. Bertini and M. Fagotti, Determination of the Nonequilibrium Steady State Emerging from a Defect, *Phys. Rev. Lett.* **117**, 130402 (2016).
  - [32] S. Bocini, Connected correlations in partitioning protocols: A case study and beyond, *SciPost Phys.* **15**, 027 (2023).
  - [33] V. Zauner, M. Ganahl, H. G. Evertz, and T. Nishino, Time evolution within a comoving window: scaling of signal fronts and magnetization plateaus after a local quench in quantum spin chains, *Journal of Physics:*

- Condensed Matter **27**, 425602 (2015).
- [34] G. Delfino and M. Sorba, Space of initial conditions and universality in nonequilibrium quantum dynamics, Nuclear Physics B **983**, 115910 (2022).
  - [35] B. Bertini, M. Fagotti, L. Piroli, and P. Calabrese, Entanglement evolution and generalised hydrodynamics: noninteracting systems, Journal of Physics A: Mathematical and Theoretical **51**, 39LT01 (2018).
  - [36] M. Fagotti and V. Marić, Asymptotic behaviour of determinants through the expansion of the Moyal star product, arXiv:2406.12781 [math-ph].
  - [37] F. Ares, S. Murciano, and P. Calabrese, Entanglement asymmetry as a probe of symmetry breaking, Nat Commun **2036** (2023).
  - [38] F. Fröwis, P. Sekatski, W. Dür, N. Gisin, and N. Sangouard, Macroscopic quantum states: Measures, fragility, and implementations, Rev. Mod. Phys. **90**, 025004 (2018).
  - [39] I. Frérot and T. Roscilde, Quantum variance: A measure of quantum coherence and quantum correlations for many-body systems, Phys. Rev. B **94**, 075121 (2016).
  - [40] M. Fagotti, Charges and currents in quantum spin chains: late-time dynamics and spontaneous currents, J. Phys. A: Math. Theor. **50**, 034005 (2016).
  - [41] M. Gaudin, Une démonstration simplifiée du théorème de Wick en mécanique statistique, Nuclear Physics **15**, 89 (1960).
  - [42] If a state is  $\kappa$ -site shift invariant, the symbol is a  $2\kappa$ -by- $2\kappa$  matrix function of the momentum.
  - [43] E. Bettelheim and P. B. Wiegmann, Universal Fermi distribution of semiclassical nonequilibrium Fermi states, Phys. Rev. B **84**, 085102 (2011).
  - [44] D. S. Dean, P. Le Doussal, S. N. Majumdar, and G. Schehr, Wigner function of noninteracting trapped fermions, Phys. Rev. A **97**, 063614 (2018).
  - [45] E. H. Lieb and D. W. Robinson, The finite group velocity of quantum spin systems, Commun. Math. Phys. **28**, 251 (1972).
  - [46] S. Bravyi, M. B. Hastings, and F. Verstraete, Lieb-Robinson Bounds and the Generation of Correlations and Topological Quantum Order, Phys. Rev. Lett. **97**, 050401 (2006).
  - [47] M. Fagotti, Local conservation laws in spin-xy chains with open boundary conditions, Journal of Statistical Mechanics: Theory and Experiment **2016**, 063105 (2016).
  - [48] P. Calabrese, F. H. L. Essler, and M. Fagotti, Quantum quench in the transverse field Ising chain: I. Time evolution of order parameter correlators, Journal of Statistical Mechanics: Theory and Experiment **2012**, P07016 (2012).
  - [49] R. Haag, D. Kastler, and E. B. Trych-Pohlmeyer, Stability and equilibrium states, Communications in Mathematical Physics **38**, 173 (1974).
  - [50] F. Ferro, F. Ares, and P. Calabrese, Non-equilibrium entanglement asymmetry for discrete groups: the example of the XY spin chain, J. Stat. Mech. **2402**, 023101 (2024), arXiv:2307.06902 [cond-mat.stat-mech].
  - [51] L. Capizzi and M. Mazzoni, Entanglement asymmetry in the ordered phase of many-body systems: the ising field theory, Journal of High Energy Physics **2023**, 144 (2023).
  - [52] F. Ares, S. Murciano, E. Vernier, and P. Calabrese, Lack of symmetry restoration after a quantum quench: An entanglement asymmetry study, SciPost Phys. **15**, 089 (2023).
  - [53] L. Capizzi and V. Vitale, A universal formula for the entanglement asymmetry of matrix product states, arXiv:2310.01962 [quant-ph] (2024).
  - [54] F. Caceffo, S. Murciano, and V. Alba, Entangled multiplets, asymmetry, and quantum mpemba effect in dissipative systems, Journal of Statistical Mechanics: Theory and Experiment **2024**, 063103 (2024).
  - [55] L. K. Joshi, J. Franke, A. Rath, F. Ares, S. Murciano, F. Kranzl, R. Blatt, P. Zoller, B. Vermersch, P. Calabrese, C. F. Roos, and M. K. Joshi, Observing the quantum mpemba effect in quantum simulations, Phys. Rev. Lett. **133**, 010402 (2024).
  - [56] C. Rylands, K. Klobas, F. Ares, P. Calabrese, S. Murciano, and B. Bertini, Microscopic origin of the quantum mpemba effect in integrable systems, Phys. Rev. Lett. **133**, 010401 (2024).
  - [57] S. Murciano, F. Ares, I. Klich, and P. Calabrese, Entanglement asymmetry and quantum mpemba effect in the xy spin chain, Journal of Statistical Mechanics: Theory and Experiment **2024**, 013103 (2024).
  - [58] B. J. J. Khor, D. M. Kürkçioğlu, T. J. Hobbs, G. N. Perdue, and I. Klich, Confinement and kink entanglement asymmetry on a quantum ising chain, Quantum **8**, 1462 (2024).
  - [59] K. Klobas, Non-equilibrium dynamics of symmetry-resolved entanglement and entanglement asymmetry: Exact asymptotics in rule 54, arXiv:2407.21793 [cond-mat.stat-mech] (2024).
  - [60] M. Chen and H.-H. Chen, Rényi entanglement asymmetry in  $(1+1)$ -dimensional conformal field theories, Phys. Rev. D **109**, 065009 (2024).
  - [61] M. Fagotti and P. Calabrese, Entanglement entropy of two disjoint blocks in XY chains, Journal of Statistical Mechanics: Theory and Experiment **2010**, P04016 (2010).
  - [62] M. Fagotti, Global Quenches after Localized Perturbations, Phys. Rev. Lett. **128**, 110602 (2022).
  - [63] K. Bidzhiev, M. Fagotti, and L. Zadnik, Macroscopic Effects of Localized Measurements in Jammed States of Quantum Spin Chains, Phys. Rev. Lett. **128**, 130603 (2022).
  - [64] L. Zadnik, S. Bocini, K. Bidzhiev, and M. Fagotti, Measurement catastrophe and ballistic spread of charge density with vanishing current, Journal of Physics A: Mathematical and Theoretical **55**, 474001 (2022).
  - [65] M. Fagotti, Quantum Jamming Brings Quantum Mechanics to Macroscopic Scales, Phys. Rev. X **14**, 021015 (2024).
  - [66] S. Bocini and M. Fagotti, Growing Schrödinger's cat states by local unitary time evolution of product states, Phys. Rev. Res. **6**, 033108 (2024).
  - [67] G. Tóth and D. Petz, Extremal properties of the variance and the quantum Fisher information, Phys. Rev. A **87**, 032324 (2013).
  - [68] S. Yu, Quantum Fisher Information as the Convex Roof of Variance, arXiv:1302.5311 [quant-ph] (2013).
  - [69] S. Sachdev and A. P. Young, Low Temperature Relaxational Dynamics of the Ising Chain in a Transverse Field, Phys. Rev. Lett. **78**, 2220 (1997).
  - [70] With the level of approximation we are working on, we can make the identification  $P_{((z_0, z_0+dz_0))} \nearrow^{(z_1, z_2)} \sim$

- $P((z_0, z_0+dz_0) \nearrow^{(z_1, \infty)}) - P((z_0, z_0+dz_0) \nearrow^{(z_2, \infty)})$ .
- [71] G. Vidal and R. F. Werner, Computable measure of entanglement, *Phys. Rev. A* **65**, 032314 (2002).
  - [72] M. B. Plenio, Logarithmic negativity: A full entanglement monotone that is not convex, *Phys. Rev. Lett.* **95**, 090503 (2005).
  - [73] A. Coser, E. Tonni, and P. Calabrese, Entanglement negativity after a global quantum quench, *Journal of Statistical Mechanics: Theory and Experiment* **2014**, P12017 (2014).
  - [74] X. Wen, P.-Y. Chang, and S. Ryu, Entanglement negativity after a local quantum quench in conformal field theories, *Phys. Rev. B* **92**, 075109 (2015).
  - [75] V. Eisler and Z. Zimborás, On the partial transpose of fermionic gaussian states, *New Journal of Physics* **17**, 053048 (2015).
  - [76] M. Gruber and V. Eisler, Time evolution of entanglement negativity across a defect, *Journal of Physics A: Mathematical and Theoretical* **53**, 205301 (2020).
  - [77] V. Eisler, Entanglement negativity in a nonequilibrium steady state, *Phys. Rev. B* **107**, 075157 (2023).
  - [78] B. Bertini, K. Klobas, and T.-C. Lu, Entanglement negativity and mutual information after a quantum quench: Exact link from space-time duality, *Phys. Rev. Lett.* **129**, 140503 (2022).
  - [79] V. Eisler and Z. Zimborás, Area-law violation for the mutual information in a nonequilibrium steady state, *Phys. Rev. A* **89**, 032321 (2014).
  - [80] M. Kormos and Z. Zimborás, Temperature driven quenches in the ising model: appearance of negative rényi mutual information, *Journal of Physics A: Mathematical and Theoretical* **50**, 264005 (2017).
  - [81] V. Alba and P. Calabrese, Entanglement dynamics after quantum quenches in generic integrable systems, *SciPost Phys.* **4**, 017 (2018).
  - [82] V. Alba and P. Calabrese, Quantum information scrambling after a quantum quench, *Phys. Rev. B* **100**, 115150 (2019).
  - [83] G. Perez and R. Bonsignori, Analytical results for the entanglement dynamics of disjoint blocks in the xy spin chain, *Journal of Physics A: Mathematical and Theoretical* **55**, 505005 (2023).
  - [84] F. Caceffo and V. Alba, Negative tripartite mutual information after quantum quenches in integrable systems, *Phys. Rev. B* **108**, 134434 (2023).
  - [85] V. Marić and M. Fagotti, Universality in the tripartite information after global quenches, *Phys. Rev. B* **108**, L161116 (2023).
  - [86] V. Marić and M. Fagotti, Universality in the tripartite information after global quenches: (generalised) quantum xy models, *Journal of High Energy Physics* **2023**, 140 (2023).
  - [87] V. Marić, Universality in the tripartite information after global quenches: spin flip and semilocal charges, *Journal of Statistical Mechanics: Theory and Experiment* **2023**, 113103 (2023).
  - [88] V. Marić, S. Bocini, and M. Fagotti, Entanglement entropy of two disjoint intervals and spin structures in interacting chains in and out of equilibrium, *Journal of High Energy Physics* **2024**, 44 (2024).
  - [89] Y. Zou, K. Siva, T. Soejima, R. S. K. Mong, and M. P. Zaletel, Universal tripartite entanglement in one-dimensional many-body systems, *Phys. Rev. Lett.* **126**, 120501 (2021).
  - [90] C. Berthiere, Tripartite entanglement dynamics following a quantum quench, *arXiv:2408.12533 [cond-mat.stat-mech]* (2024).
  - [91] M. Dalmonte, V. Eisler, M. Falconi, and B. Vermersch, Entanglement hamiltonians: From field theory to lattice models and experiments, *Annalen der Physik* **534**, 2200064 (2022).
  - [92] G. D. Giulio, R. Arias, and E. Tonni, Entanglement hamiltonians in 1d free lattice models after a global quantum quench, *Journal of Statistical Mechanics: Theory and Experiment* **2019**, 123103 (2019).
  - [93] F. Rottoli, C. Rylands, and P. Calabrese, Entanglement hamiltonians and the quasiparticle picture, *arXiv:2407.01730 [quant-ph]* (2024).
  - [94] F. H. L. Essler and R. M. Konik, Finite-temperature lineshapes in gapped quantum spin chains, *Phys. Rev. B* **78**, 100403 (2008).
  - [95] E. Granet, M. Fagotti, and F. H. L. Essler, Finite temperature and quench dynamics in the Transverse Field Ising Model from form factor expansions, *SciPost Phys.* **9**, 033 (2020).
  - [96] F. Fazio, J. Keeling, L. Mazza, and M. Schirò, Many-body open quantum systems, *arXiv:2409.10300 [quant-ph]* (2024).
  - [97] M. Gibbins, A. Jafarizadeh, A. Gammon-Smith, and B. Bertini, Quench dynamics in lattices above one dimension: The free fermionic case, *Phys. Rev. B* **109**, 224310 (2024).
  - [98] S. Yamashika, F. Ares, and P. Calabrese, Entanglement asymmetry and quantum mpemba effect in two-dimensional free-fermion systems, *Phys. Rev. B* **110**, 085126 (2024).
  - [99] F. Balducci, A. Gambassi, A. Lerose, A. Scardicchio, and C. Vanoni, Localization and melting of interfaces in the two-dimensional quantum ising model, *Phys. Rev. Lett.* **129**, 120601 (2022).
  - [100] F. Balducci, A. Gambassi, A. Lerose, A. Scardicchio, and C. Vanoni, Interface dynamics in the two-dimensional quantum ising model, *Phys. Rev. B* **107**, 024306 (2023).
  - [101] L. Pavešić, D. Jaschke, and S. Montangero, Constrained dynamics and confinement in the two-dimensional quantum ising model, *arXiv:2406.11979 [quant-ph]* (2024).